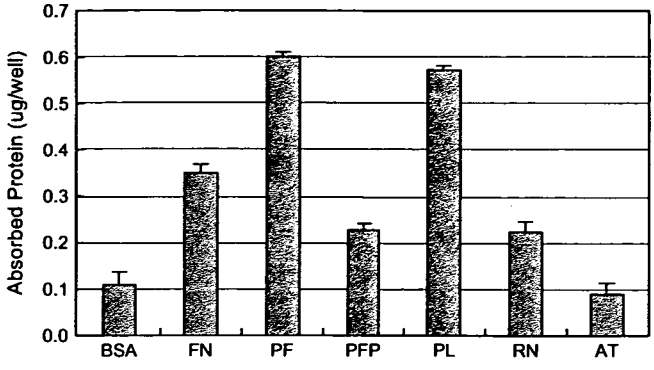

Fig. 3. Protein absorption on non-treated polystyrene plates. Ten μg/ml of bovine serum albumin (BSA), Fibronectin (FN), Pronectin F (PF), Pronectin F PLUS (PFP), Pronectin L (PL), Retronectin (RN) or Attachin (AN) was added to 96-well plates and incubated at room temperature for 2 h. Each well was washed with PBS(−) and the amount of absorbed protein was quantitated by QuantiPro BCA using bovine serum albumin as a standard. Each data point represents the mean ± S.D. of triplicate determinations.

media. Similar results were obtained when the cells were stimulated with thrombin (Fig. 6B).

Next, t-PA production from the thrombin-stimulated HUVECs was examined. As shown in Fig. 7, the t-PA concentration in the culture supernatant of HUVECs that adhered on Pronectin F PLUS was the same as that on Fibronectin. However, the concentration was lower in the supernatant on Pronectin F, Retronectin, or Attachin than on fibronectin. The basal production of t-PA in the serum-free media was less than in growing media; therefore, responsiveness to thrombin was readily observed in the serum-free culture.

During these experiments using thrombin, detachment of the thrombin-stimulated cells from Pronectin F, Retronectin, or Attachin was observed (Fig. 8). No detachment was seen in the cells that adhered on fibronectin or Pronectin F PLUS. This result might reflect the possibility that the adhesiveness of the cells to Pronectin F, Retronectin, and Attachin is weaker than to Pronectin F PLUS or fibronectin.

The following data support the results of Fig. 8, which are presented using microscopic images. Since HUVECs are adherent cells, detachment from the dishes leads to a loss of viability. Therefore, changes in the viable cell concentration after thrombin stimulation reflect cell detachment. As shown in Fig. 9, the production of t-PA and changes in the viable cell concentration after culturing in the presence of 0.01, 0.1, or 1 U/ml of thrombin were tested. At all three concentrations of thrombin used, cell detachment was observed only from Pronectin F. Although the t-PA concentration was increased in a dose-dependent manner by thrombin in the cells that adhered on Fibronectin or Pronectin F PLUS (Fig. 9A), there was less of an increase in t-PA production from the cells on Pronectin F when a low dose (0.01 or 0.1 U/ml) of thrombin was used. At those concentrations, the viable cell concentration on Pronectin F was decreased by thrombin stimulation, meaning that cell detachment occurred on Pronectin F (Fig. 9B). At a high concentration of thrombin (1 U/ml), the viable cell concentration decreased slightly even though cell detachment was

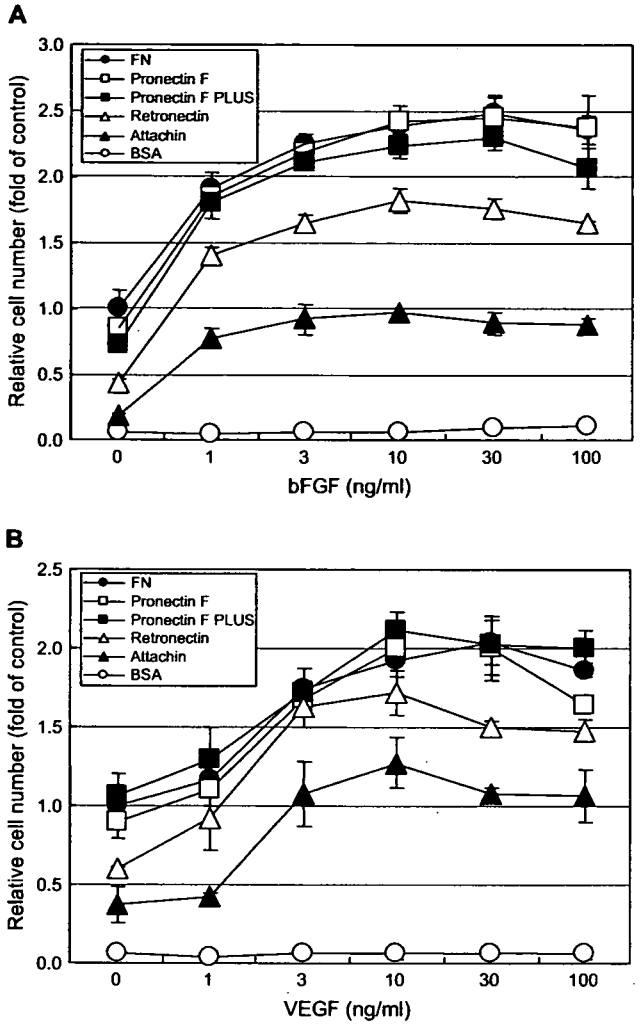

Fig. 4. Effects of recombinant cell adhesive proteins on the VEGF- or bFGF-induced cell proliferation. HUVECs were seeded into wells previously coated with 10 μg/ml of Fibronectin, Pronectin F, Pronectin F PLUS, Retronectin, Attachin, or BSA, and cultured for 2 days in the presence or absence of bFGF (A) or VEGF (B) at the concentrations indicated. The relative cell number was examined using a cell counting kit-8. The results are expressed as the mean value ± S.D. of triplicate determinations.

observed. This might be because the cell proliferative effect of thrombin canceled the decrease in cell viability. t-PA production corrected by the viable cell concentration is shown in Fig. 9C. By correcting the t-PA concentration using the viable cell concentration, the dose-dependency of thrombin in t-PA production was similar in Pronectin F to Pronectin F PLUS and fibronectin (Fig. 9C). From these results, in the cells on Pronectin F and Pronectin F PLUS, the signals from thrombin transduced similarly, but the strength of the cell adhesion differed.

4. Discussion

The goal of the present study was to establish a cell culture method that can improve the safety of cellular therapy products. Our focus is now on human endothelial cells, because

Please cite this article in press as: Ishii-Watabe A et al., Influences of the recombinant artificial cell adhesive proteins on the behavior of human umbilical vein endothelial cells in serum-free culture, Biologicals (2007), doi:10.1016/j.biologicals.2006.12.002

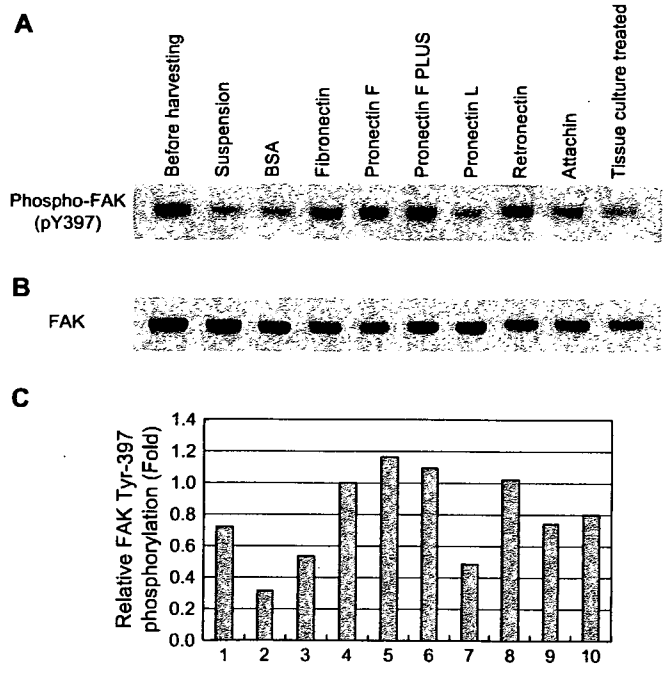

Fig. 5. FAK activation in HUVECs adhered to recombinant cell adhesive proteins. HUVECs cultured in serum-containing EGM-2 media on collagen-coated plates were harvested and held in suspension for 2 h at 37 °C, then plated onto precoated plates with 10 μg/ml of Fibronectin, Pronectin F, Pronectin F PLUS, Pronectin L, Retronectin, or Attachin. After 2 h incubation at 37 °C, cell lysates were prepared using RIPA buffer. The cell extracts were analyzed for the phosphorylation (A) and protein levels of focal adhesion kinase (B) by Western blotting. The amount of proteins detected was analyzed using MultiGauge software (C). Lane 1: before harvesting; lane 2: after suspension; lane 3: BSA; lane 4: Fibronectin; lane 5: Pronectin F; lane 6: Pronectin F PLUS; lane 7: Pronectin L; lane 8: Retronectin; lane 9: Attachin; lane 10: tissue culture-treatment dish. Similar results were obtained in two independent experiments. Representative blots are shown.

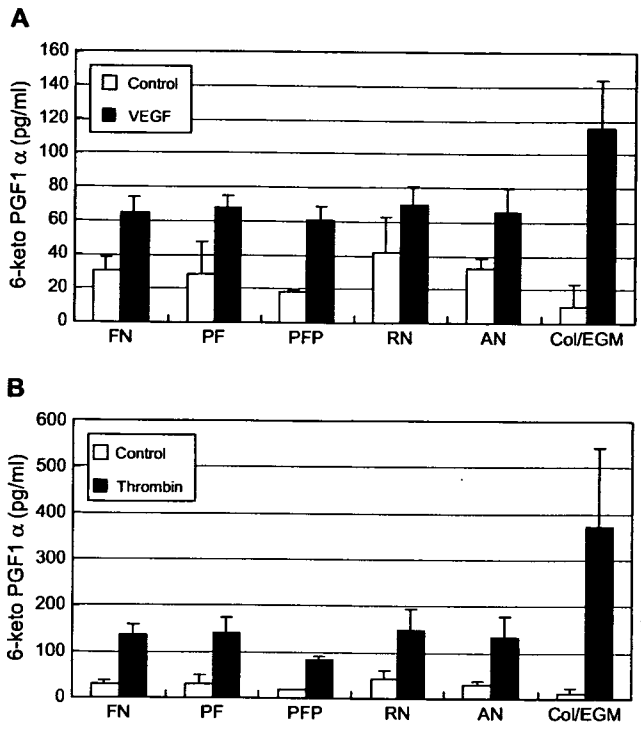

Fig. 6. Effects of cell adhesive proteins on the VEGF- or thrombin- stimulated production of Prostaglandin I_2. HUVECs were seeded at 7×10^4 cells/well on 24-well plates previously coated with Fibronectin (FN), Pronectin F (PF), Pronectin F PLUS (PFP), Retronectin (RN), or Attachin (AN). After culturing for 1 day, the cells were stimulated with 30 ng/ml of VEGF (A) or 1 U/ml of thrombin (B). One hour later, the conditioned media were collected and 6-keto $PGF_1\alpha$ concentration was determined by enzyme immunoassay. Results are expressed as picograms of $PGF_1\alpha$/ml of the supernatant and represent the mean ± S.D. of triplicate determinations. 6-Keto $PGF_1\alpha$ production from HUVECs cultured in serum-containing growing media (EGM-2) plated on a collagen-coated dish was also examined (Col/EGM).

they are expected to be put into clinical use in the near future. Serum-free culture supplemented with recombinant proteins produced without using animal-derived materials would be optimal in order to avoid contamination by animal-derived materials and transmissible agents. This work was carried out as a step in demonstrating the feasibility of recombinant cell adhesion proteins in serum-free cultures of human endothelial cells, which might form the basis of future cellular therapies. HUVECs were used as a model of tissue-derived differentiated endothelial cells.

One of the uses of endothelial cells in cellular therapy is for the vascularization of engineered tissue. Vascularization of a tissue-engineered construct is mediated primarily through the ingrowth of surrounding vessels from the peri-implant tissue. However, this process is quite slow and is not sufficient to achieve appropriate vascularization of large defects [32]. The incorporation of endothelial cells or vascular-like structure in the tissue-engineered constructs before transplantation is a possible solution of this problem. Both human embryonic stem cell-derived endothelial cells and tissue-derived endothelial cells such as HUVECs have been shown to incorporate successfully into engineered skeletal muscle tissue [33–35]. Tissue-derived human endothelial cells are also used for the endothelialization of artificial artery grafts [36]. Although serum-free media for human endothelial cells has been developed, being supplemented with a cell adhesion protein such as fibronectin is necessary [26]. Since plasma fibronectin is known to bind to several pathogens including viruses [37,38], use of a recombinant cell adhesion protein would be desired in order to avoid the contamination of infectious agents.

Another use of endothelial cells in cellular therapy is for therapeutic neovascularization, an important adaptation to rescue tissue from critical ischemia. In a rat model of myocardial infarction, transplantation of HUVECs has been shown to contribute to increased neovascularization [39]. Recently, much attention has been paid to outgrowth endothelial cells (OECs) obtained by *in vitro* culture of blood mononuclear cells [40–46]. OECs show a marked similarity to fully differentiated endothelial cells with respect to their cellular morphology, marker expression and potential to form capillary-like structures [43,44,47]. Because OECs can be obtained from blood mononuclear cells, they have the advantage that autologous endothelial cells could be obtained without invasive procedures. The potential use of OECs for therapeutic neovascularization has been shown in murine ischemia models

Please cite this article in press as: Ishii-Watabe A et al. Influences of the recombinant artificial cell adhesive proteins on the behavior of human umbilical vein endothelial cells in serum-free culture, Biologicals (2007), doi:10.1016/j.biologicals.2006.12.002

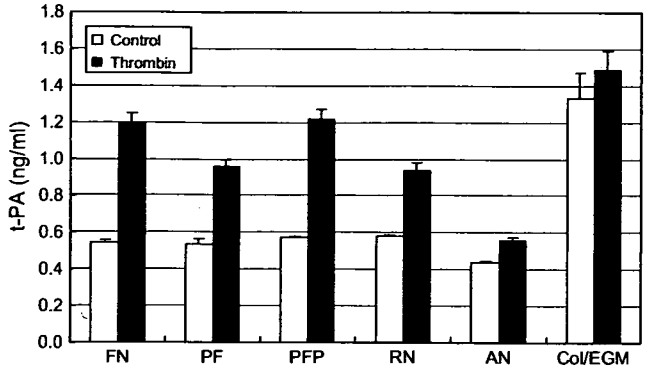

Fig. 7. Effects of cell adhesive proteins on the thrombin- stimulated production of tissue plasminogen activator. HUVECs were seeded at 7 × 10^4 cells/well on 24-well plates previously coated with Fibronectin (FN), Pronectin F (PF), Pronectin F PLUS (PFP), Retronectin (RN), or Attachin (AN). After culturing for 1 day, the cells were stimulated with 1 U/ml of thrombin. After 24 h incubation, the conditioned media were collected and t-PA concentration was determined by enzyme immunoassay. Results are expressed as nanograms of t-PA/ml of the supernatant and represent the mean ± S.D. of triplicate determinations. t-PA production from HUVECs cultured in serum-containing growing media (EGM-2) plated on collagen-coated dish was also examined (Col/EGM).

[47–50]. The culture conditions for OECs and for tissue-derived endothelial cells such as HUVECs are the same: endothelial basal media supplemented with fetal calf serum, VEGF, basic FGF, IGF-1, EGF and ascorbic acid. Fibronectin is the cell adhesion protein most commonly used to obtain OECs. Therefore, examining the usefulness of recombinant cell adhesion proteins as a substitute for plasma fibronectin in serum-free culture would lead to the establishment of a serum-free culture for OECs as well.

The cell culture method chosen has a direct influence on the quality and safety of cellular therapy products. The composition of media and serum are considered to affect the features of the cells, and animal-derived materials are known to carry the risk of infection or allergy. Thus, developing appropriate culture methods and ways of evaluating these methods are key to assuring the safety of cellular therapy products [11,12]. For example, when culturing human embryonic stem cells that are anticipated to be a useful source for cellular therapy products, non-human-type sialic acid (*N*-glycolyl neuraminic acid) derived from animal serum is incorporated into the sugar chain on the cell surface, which could induce an immune response

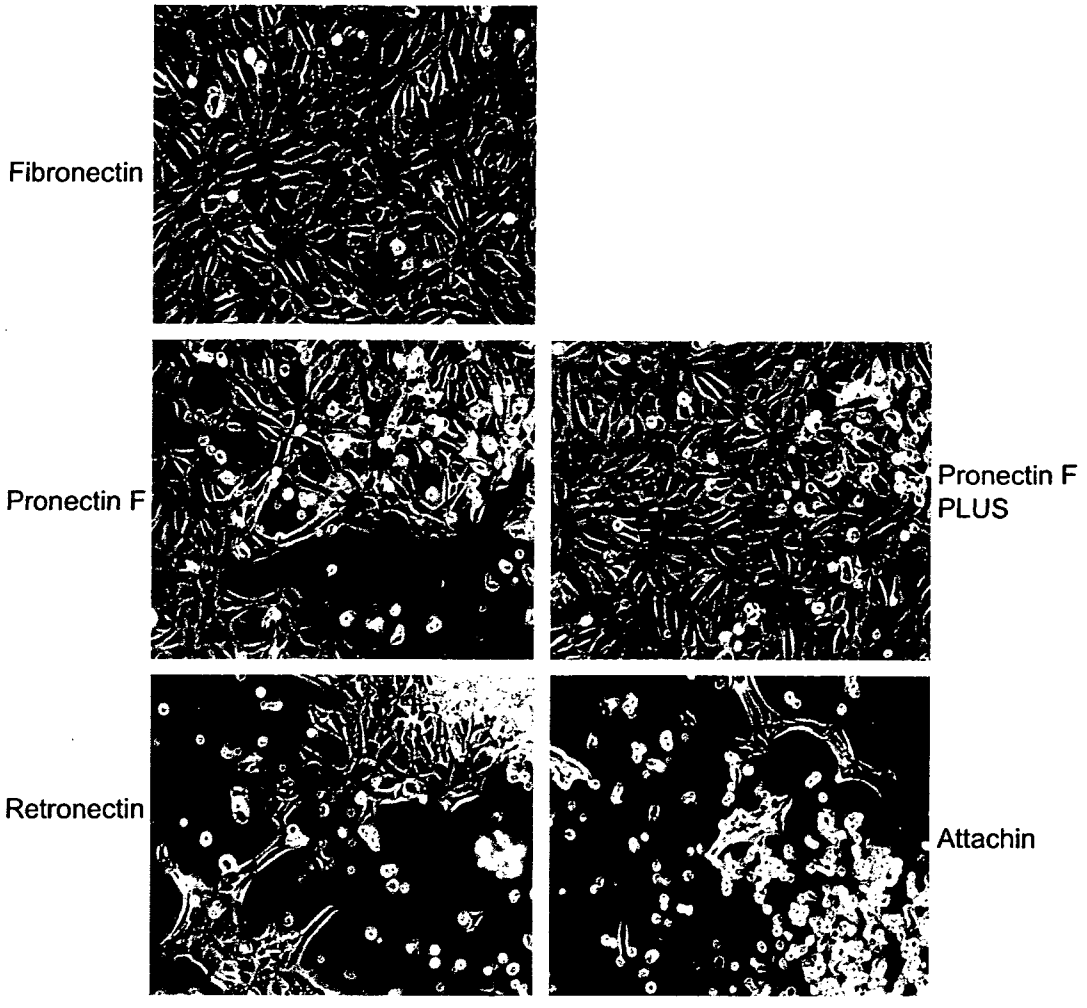

Fig. 8. Detachment of HUVECs cultured in the presence of thrombin. Cells were plated on the plates previously coated with Fibronectin, Pronectin F, Pronectin F PLUS, Retronectin, or Attachin, and cultured for 24 h in the presence of 1 U/ml of thrombin. The cells were photographed before harvesting the supernatant that is provided for the measurement of the t-PA concentration.

Please cite this article in press as: Ishii-Watabe A et al., Influences of the recombinant artificial cell adhesive proteins on the behavior of human umbilical vein endothelial cells in serum-free culture, Biologicals (2007), doi:10.1016/j.biologicals.2006.12.002

upon transplantation [51]. In addition, the transmission of unknown viruses from rodent feeder cells is also a concern [8]. Therefore, establishing cell culture methods that assure safety is an important goal in the development of cellular therapy products.

Because recombinant proteins can be produced without using animal or human-derived materials, providing the protein factors that are necessary to cell culture as recombinant proteins can contribute to improving the safety of cellular therapy products. Recombinant proteins also have an advantage in that they can provide consistent performance from lot to lot, and their function can be modified by molecular design. Artificial recombinant proteins have the possibility of being superior to naturally occurring proteins; for example, Retronectin, a deletion mutant of fibronectin that unfortunately showed less activity as an adhesive protein in this study, is much more effective in supporting gene transfer by retrovirus vectors than fibronectin [23]. If there is a concern in using artificial recombinant proteins, the residual artificial protein has the potential to show immunogenicity.

In our experiments to test cell adhesion, Pronectin F and Pronectin F PLUS were superior to fibronectin when they were used in lower concentrations (Fig. 1). This might be because both Pronectin F and Pronectin F PLUS have 13 repeats of the RGD sequence in one molecule, whereas fibronectin has only two. Pronectin F and Pronectin F PLUS are also structurally stable, and thus the coated substrates retain their performance for at least 2 years at room temperature, which is another advantage over fibronectin [52]. Pronectins were produced without using any animal-derived components (Dr. Kurokawa, Sanyo Kasei Kogyo, personal communication).

Pronectin F is not soluble in water since the silk-like protein sequence forms strong hydrogen bonds intermolecularly; thus, it must be dissolved in $LiClO_4$ [21]. Therefore, Pronectin F PLUS, a water-soluble variant of Pronectin F, was developed by chemical modification of the serine residues of Pronectin F [22]. As shown in Fig. 3, a higher amount of Pronectin F was absorbed on polystyrene dishes than Pronectin F PLUS. Since the surface of polystyrene plates is hydrophobic, hydrophobic Pronectin F might have been absorbed well. Pronectin L, which has a similar core sequence to that of Pronectin F, was also absorbed well on the dish, although no cells adhered on it.

In spite of their differences in absorption on the polystyrene dish, Pronectin F PLUS and Pronectin F showed similar efficiency with respect to the adhered cell number, growth support, induction of FAK phosphorylation, and production of PGI_2 and t-PA. Moreover, Pronectin F PLUS was more potent than Pronectin F in its support of cell adhesion under stimulation with thrombin (Fig. 9). The cells on Pronectin F PLUS were resistant to cell detachment due to the thrombin-induced cytoskeletal changes. This might be because that Pronectin F PLUS is positively charged by chemical modification. Since the cell surface possesses a negative charge, the adhesive intensity between the cells and Pronectin F PLUS was increased due to the static electrical interaction, resulting in the maintenance of cell adhesiveness after the cytoskeletal change

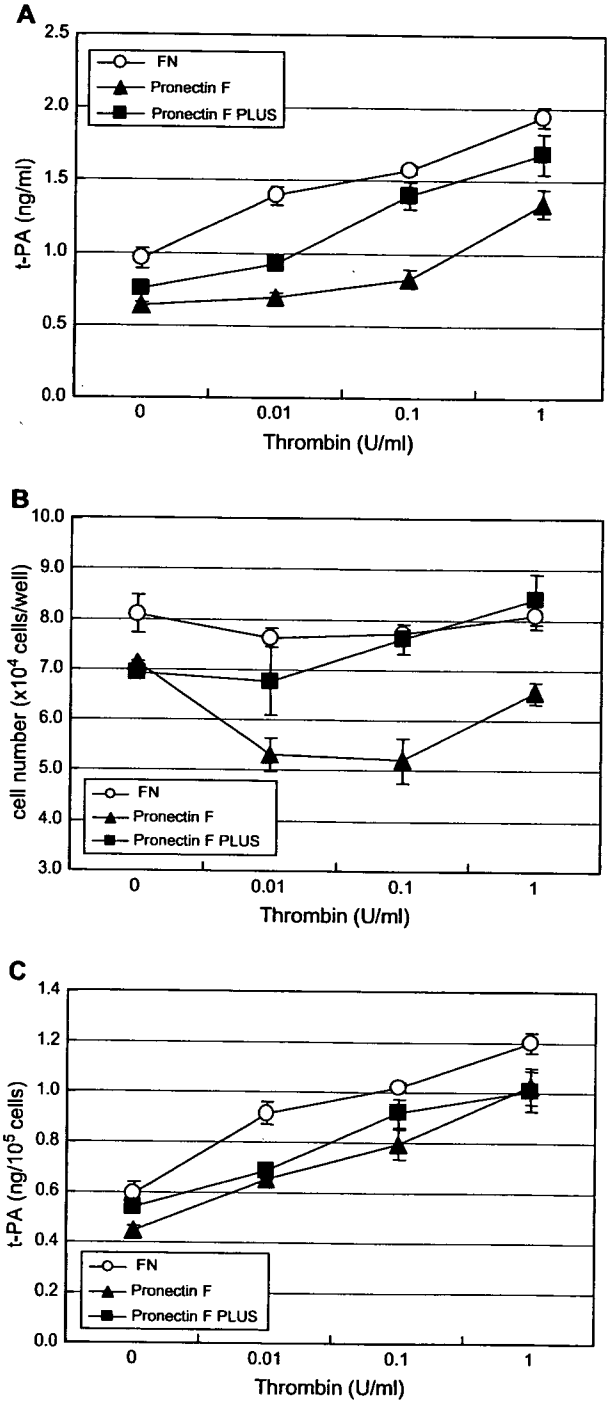

Fig. 9. Thrombin-induced production of t-PA and decrease in viability of HUVECs adhered on Pronectin F. HUVECs were seeded at 7×10^4 cells/well on 24-well plates previously coated with Fibronectin, Pronectin F or Pronectin F PLUS. After culturing for 1 day, the cells were stimulated with thrombin at the indicated concentrations. After 24 h incubation, the conditioned media were collected and t-PA concentration was determined by enzyme immunoassay (A). The cell numbers were determined using a Cell-Counting Kit-8 (B). Production of t-PA per 10^5 cells was calculated (C). Each data point represents the mean ± S.D. of triplicate determinations.

Please cite this article in press as: Ishii-Watabe A et al., Influences of the recombinant artificial cell adhesive proteins on the behavior of human umbilical vein endothelial cells in serum-free culture, Biologicals (2007), doi:10.1016/j.biologicals.2006.12.002

induced by thrombin. To our knowledge, this is the first observation to reveal the difference in biological properties between Pronectin F and Pronectin F PLUS. The retention of human endothelial cells on the lumen in the presence of physiological stimuli is an important prerequisite for artificial artery grafts to be successful, and, therefore, Pronectin F PLUS could also be suited for use in this type of graft.

In the present study, the usefulness of Pronectin F PLUS as a substitute for fibronectin was indicated; however, Pronectin F PLUS and Pronectin F were less effective than fibronectin in long-term cell cultures. We were able to culture HUVECs up to around 6 passages using the serum-free media with fibronectin. However, when Pronectin F or Pronectin F PLUS was used instead of fibronectin, the cell number did not increase beyond the second passage. Although Pronectin F PLUS worked better than Pronectin F, the efficiency of both was lower than that of fibronectin in the long-term maintenance of HUVECs. Since fibronectin has several functional domains that can bind to heparin, fibrin and collagen, signals other than the RGD-integrin interaction would be important in the long-term maintenance of the cells. The incorporation of domains other than that of RGD of fibronectin into Pronectin F PLUS would be necessary to improve its efficacy in long-term cell cultures.

For cell cultures, porcine trypsin is often used when cells are harvested. The use of trypsin may lead to the contamination of animal-derived materials or transmissible agents. In serum-free cultures of HUVECs, we were able to harvest cells for passage using a protease free of animal-derived materials such as TrypLE Select (Invitrogen, Carlsbad, CA, USA) or AccuMax (Chemicon, Billerica, MA, USA); therefore, trypsin is not necessarily used for the maintenance of HUVECs, which means that it is possible to eliminate the potential for contamination of animal-derived proteins.

In summary, Pronectin F PLUS was shown to have the closest activity to plasma fibronectin in the serum-free culture of HUVECs by examining VEGF- or bFGF-induced cell proliferation, FAK phosphorylation, and thrombin-stimulated production of PGI_2 or t-PA. The cell adherent activity of Pronectin F PLUS was superior to fibronectin at concentrations of less than 1 μg/ml. Although Pronectin F PLUS has the same amino acid sequence as Pronectin F, only HUVECs on Pronectin F PLUS were resistant to thrombin-induced cell detachment. Pronectin F PLUS is thus thought to be a promising substitute for plasma fibronectin in the serum-free culture of endothelial cells, although modification would be necessary to improve its efficiency in long-term cell cultures.

Acknowledgements

This work was supported in part by a Grant-in-Aid for Health and Labor Science Research (H17-SAISEI-021 and H17-IYAKU-015) from the Japanese Ministry of Health, Labor and Welfare, and a Grant-in-Aid for Young Scientists (B) from the Ministry of Education, Science, Sports and Culture.

References

[1] Wollert KC, Drexler H. Cell-based therapy for heart failure. Curr Opin Cardiol 2006;21:234–9.
[2] Zavos PM. Stem cells and cellular therapy: potential treatment for cardiovascular diseases. Int J Cardiol 2006;107:1–6.
[3] Fazel S, Tang GH, Angoulvant D, Cimini M, Weisel RD, Li RK, et al. Current status of cellular therapy for ischemic heart disease. Ann Thorac Surg 2005;79:S2238–47.
[4] http://www.fda.gov/cber/gdlns/somgene.pdf.
[5] http://www.fda.gov/cber/gdlns/cmcsomcell.pdf.
[6] http://www.emea.eu.int/pdfs/human/cpwp/32377405en.pdf.
[7] http://www.fda.gov/cber/rules/suitdonor.pdf.
[8] Lee JB, Lee JE, Park JH, Kim SJ, Kim MK, Roh SI, et al. Establishment and maintenance of human embryonic stem cell lines on human feeder cells derived from uterine endometrium under serum-free condition. Biol Reprod 2005;72:42–9.
[9] Ogawa K, Matsui H, Ohtsuka S, Niwa H. A novel mechanism for regulating clonal propagation of mouse ES cells. Genes Cells 2004;9:471–7.
[10] Asher DM. Bovine sera used in the manufacture of biologicals: current concerns and policies of the U.S. Food and Drug Administration regarding the transmissible spongiform encephalopathies. Dev Biol Stand 1999; 99:41–4.
[11] Asher DM. The transmissible spongiform encephalopathy agents: concerns and responses of United States regulatory agencies in maintaining the safety of biologics. Dev Biol Stand 1999;100:103–18.
[12] Cobo F, Stacey GN, Hunt C, Cabrera C, Nieto A, Montes R, et al. Microbiological control in stem cell banks: approaches to standardisation. Appl Microbiol Biotechnol 2005;68:456–66.
[13] Cobo F, Talavera P, Concha A. Diagnostic approaches for viruses and prions in stem cell banks. Virology 2006;347:1–10.
[14] Kornblihtt AR, Umezawa K, Vibe-Pedersen K, Baralle FE. Primary structure of human fibronectin: differential splicing may generate at least 10 polypeptides from a single gene. EMBO J 1985;4:1755–9.
[15] Umezawa K, Kornblihtt AR, Baralle FE. Isolation and characterization of cDNA clones for human liver fibronectin. FEBS Lett 1985;186:31–4.
[16] Pierschbacher MD, Ruoslahti E. Cell attachment activity of fibronectin can be duplicated by small synthetic fragments of the molecule. Nature 1984;309:30–3.
[17] Ruoslahti E, Pierschbacher MD. New perspectives in cell adhesion: RGD and integrins. Science 1987;238:491–7.
[18] Bourdoulous S, Orend G, MacKenna DA, Pasqualini R, Ruoslahti E. Fibronectin matrix regulates activation of RHO and CDC42 GTPases and cell cycle progression. J Cell Biol 1998;143:267–76.
[19] Frisch SM, Ruoslahti E. Integrins and anoikis. Curr Opin Cell Biol 1997;9:701–6.
[20] Heslot H. Artificial fibrous proteins: a review. Biochimie 1998;80:19–31.
[21] Cappello J. Genetically Engineered Protein Polymers. In: Domb AJ, Kost J, Wiseman D, editors. Handbook of Biodegradable Polymers. Amsterdam: Harwood Academic Publishers; 1997. p. 387–416.
[22] Hosseinkhani H, Tabata Y. PEGylation enhances tumor targeting of plasmid DNA by an artificial cationized protein with repeated RGD sequences, Pronectin. J Control Release 2004;97:157–71.
[23] Hanenberg H, Xiao XL, Dilloo D, Hashino K, Kato I, Williams DA. Colocalization of retrovirus and target cells on specific fibronectin fragments increases genetic transduction of mammalian cells. Nat Med 1996;2:876–82.
[24] http://home.kimo.com.tw/biotaichchen/Attachin/into.html.
[25] http://home.kimo.com.tw/biotaichchen/Attachin/qa.html.
[26] Gorfien S, Spector A, DeLuca D, Weiss S. Growth and physiological functions of vascular endothelial cells in a new serum-free medium (SFM). Exp Cell Res 1993;206:291–301.
[27] Zaric J, Ruegg C. Integrin-mediated adhesion and soluble ligand binding stabilize COX-2 protein levels in endothelial cells by inducing expression and preventing degradation. J Biol Chem 2005;280:1077–85.
[28] Ilic D, Kovacic B, Johkura K, Schlaepfer DD, Tomasevic N, Han Q, et al. FAK promotes organization of fibronectin matrix and fibrillar adhesions. J Cell Sci 2004;117:177–87.

Please cite this article in press as: Ishii-Watabe A et al., Influences of the recombinant artificial cell adhesive proteins on the behavior of human umbilical vein endothelial cells in serum-free culture, Biologicals (2007), doi:10.1016/j.biologicals.2006.12.002

[29] Almeida EA, Ilic D, Han Q, Hauck CR, Jin F, Kawakatsu H, et al. Matrix survival signaling: from fibronectin via focal adhesion kinase to c-Jun NH(2)-terminal kinase. J Cell Biol 2000;149:741–54.
[30] Schlaepfer DD, Broome MA, Hunter T. Fibronectin-stimulated signaling from a focal adhesion kinase-c-Src complex: involvement of the Grb2, p130cas, and Nck adaptor proteins. Mol Cell Biol 1997;17:1702–13.
[31] Ruest PJ, Roy S, Shi E, Mernaugh RL, Hanks SK. Phosphospecific antibodies reveal focal adhesion kinase activation loop phosphorylation in nascent and mature focal adhesions and requirement for the autophosphorylation site. Cell Growth Differ 2000;11:41–8.
[32] Fuchs S, Motta A, Migliaresi C, Kirkpatrick CJ. Outgrowth endothelial cells isolated and expanded from human peripheral blood progenitor cells as a potential source of autologous cells for endothelialization of silk fibroin biomaterials. Biomaterials 2006;27:5399–408.
[33] Jain RK, Au P, Tam J, Duda DG, Fukumura D. Engineering vascularized tissue. Nat Biotechnol 2005;23:821–3.
[34] Levenberg S, Rouwkema J, Macdonald M, Garfein ES, Kohane DS, Darland DC, et al. Engineering vascularized skeletal muscle tissue. Nat Biotechnol 2005;23:879–84.
[35] Koike N, Fukumura D, Gralla O, Au P, Schechner JS, Jain RK. Tissue engineering: creation of long-lasting blood vessels. Nature 2004;428:138–9.
[36] Meinhart JG, Schense JC, Schima H, Gorlitzer M, Hubbell JA, Deutsch M, et al. Enhanced endothelial cell retention on shear-stressed synthetic vascular grafts precoated with RGD-cross-linked fibrin. Tissue Eng 2005;11:887–95.
[37] Julkunen I, Hautanen A, Keski-Oja J. Interaction of viral envelope glycoproteins with fibronectin. Infect Immun 1983;40:876–81.
[38] Torre D, Pugliese A, Ferrario G, Marietti G, Forno B, Zeroli C. Interaction of human plasma fibronectin with viral proteins of human immunodeficiency virus. FEMS Immunol Med Microbiol 1994;8:127–31.
[39] Merx MW, Zernecke A, Liehn EA, Schuh A, Skobel E, Butzbach B, et al. Transplantation of human umbilical vein endothelial cells improves left ventricular function in a rat model of myocardial infarction. Basic Res Cardiol 2005;100:208–16.
[40] Fuchs S, Hermanns MI, Kirkpatrick CJ. Retention of a differentiated endothelial phenotype by outgrowth endothelial cells isolated from human peripheral blood and expanded in long-term cultures. Cell Tissue Res 2006;326:79–92.
[41] Cai H, Gehrig P, Scott TM, Zimmermann R, Schlapbach R, Zisch AH. MnSOD marks cord blood late outgrowth endothelial cells and accompanies robust resistance to oxidative stress. Biochem Biophys Res Commun 2006;350:364–9.
[42] Sharpe 3rd EE, Teleron AA, Li B, Price J, Sands MS, Alford K, et al. The origin and in vivo significance of murine and human culture-expanded endothelial progenitor cells. Am J Pathol 2006;168:1710–21.
[43] Gulati R, Jevremovic D, Peterson TE, Chatterjee S, Shah V, Vile RG, et al. Diverse origin and function of cells with endothelial phenotype obtained from adult human blood. Circ Res 2003;93:1023–5.
[44] Lin Y, Weisdorf DJ, Solovey A, Hebbel RP. Origins of circulating endothelial cells and endothelial outgrowth from blood. J Clin Invest 2000; 105:71–7.
[45] Smadja DM, Bieche I, Uzan G, Bompais H, Muller L, Boisson-Vidal C, et al. PAR-1 activation on human late endothelial progenitor cells enhances angiogenesis in vitro with upregulation of the SDF-1/CXCR4 system. Arterioscler Thromb Vasc Biol 2005;25:2321–7.
[46] Eggermann J, Kliche S, Jarmy G, Hoffmann K, Mayr-Beyrle U, Debatin KM, et al. Endothelial progenitor cell culture and differentiation in vitro: a methodological comparison using human umbilical cord blood. Cardiovasc Res 2003;58:478–86.
[47] Hur J, Yoon CH, Kim HS, Choi JH, Kang HJ, Hwang KK, et al. Characterization of two types of endothelial progenitor cells and their different contributions to neovasculogenesis. Arterioscler Thromb Vasc Biol 2004;24:288–93.
[48] Yoon CH, Hur J, Park KW, Kim JH, Lee CS, Oh IY, et al. Synergistic neovascularization by mixed transplantation of early endothelial progenitor cells and late outgrowth endothelial cells: the role of angiogenic cytokines and matrix metalloproteinases. Circulation 2005;112: 1618–27.
[49] Ott I, Keller U, Knoedler M, Gotze KS, Doss K, Fischer P, et al. Endothelial-like cells expanded from CD34+ blood cells improve left ventricular function after experimental myocardial infarction. FASEB J 2005; 19:992–4.
[50] Choi JH, Hur J, Yoon CH, Kim JH, Lee CS, Youn SW, et al. Augmentation of therapeutic angiogenesis using genetically modified human endothelial progenitor cells with altered glycogen synthase kinase-3beta activity. J Biol Chem 2004;279:49430–8.
[51] Martin MJ, Muotri A, Gage F, Varki A. Human embryonic stem cells express an immunogenic nonhuman sialic acid. Nat Med 2005;11: 228–32.
[52] http://www.sanyo-chemical.co.jp/product/pronectin/eng/prodspec.htm.

Please cite this article in press as: Ishii-Watabe A et al. Influences of the recombinant artificial cell adhesive protcins on the behavior of human umbilical vein endothelial cells in serum-free culture. Biologicals (2007), doi:10.1016/j.biologicals.2006.12.002

Pharmaceutical Research, Vol. 24, No. 9, September 2007 (© 2007)
DOI: 10.1007/s11095-007-9296-2

Research Paper

Significance of Local Mobility in Aggregation of β-Galactosidase Lyophilized with Trehalose, Sucrose or Stachyose

Sumie Yoshioka,[1,2] Tamaki Miyazaki,[1] Yukio Aso,[1] and Tohru Kawanishi[1]

Received January 3, 2007; accepted March 14, 2007; published online April 3, 2007

Purpose. The purpose of this study is to compare the effects of global mobility, as reflected by glass transition temperature (T_g) and local mobility, as reflected by rotating-frame spin-lattice relaxation time ($T_{1\rho}$) on aggregation during storage of lyophilized β-galactosidase (β-GA).
Materials and Methods. The storage stability of β-GA lyophilized with sucrose, trehalose or stachyose was investigated at 12% relative humidity and various temperatures (40–90°C). β-GA aggregation was monitored by size exclusion chromatography (SEC). Furthermore, the $T_{1\rho}$ of the β-GA carbonyl carbon was measured by ^{13}C solid-state NMR, and T_g was measured by modulated temperature differential scanning calorimetry. Changes in protein structure during freeze drying were measured by solid-state FT-IR.
Results. The aggregation rate of β-GA in lyophilized formulations exhibited a change in slope at around T_g, indicating the effect of molecular mobility on the aggregation rate. Although the T_g rank order of β-GA formulations was sucrose < trehalose < stachyose, the rank order of β-GA aggregation rate at temperatures below and above T_g was also sucrose < trehalose < stachyose, thus suggesting that β-GA aggregation rate is not related to (T-T_g). The local mobility of β-GA, as determined by the $T_{1\rho}$ of the β-GA carbonyl carbon, was more markedly decreased by the addition of sucrose than by the addition of stachyose. The effect of trehalose on $T_{1\rho}$ was intermediate when compared to those for sucrose and stachyose. These findings suggest that β-GA aggregation rate is primarily related to local mobility. Significant differences in the second derivative FT-IR spectra were not observed between the excipients, and the differences in β-GA aggregation rate observed between the excipients could not be attributed to differences in protein secondary structure.
Conclusions. The aggregation rate of β-GA in lyophilized formulations unexpectedly correlated with the local mobility of β-GA, as indicated by $T_{1\rho}$, rather than with (T-T_g). Sucrose exhibited the most intense stabilizing effect due to the most intense ability to inhibit local protein mobility during storage.

KEY WORDS: β-galactosidase; global mobility; local mobility; lyophilized formulation; solid-state stability.

INTRODUCTION

Close correlations between storage stability and molecular mobility have been demonstrated for various lyophilized formulations of peptides and proteins (1,2). Aggregation between protein molecules is a degradation pathway commonly observed in lyophilized protein formulations. The rate of protein aggregation is generally considered to depend on the translational mobility of protein molecules, which is related to structural relaxation (α-relaxation) of the formulation. Correlations between aggregation rates and structural relaxation have been shown in various protein systems in visible ways, such as enhancement of aggregation associated with decreases in glass transition temperature (T_g) (3–6) and changes in the temperature dependence of aggregation rates around T_g (7–10). However, recent studies have suggested that molecular mobility with a length scale shorter than structural relaxation (β-relaxation or local mobility), rather than structural relaxation, is critical to protein aggregation (11,12).

The rate of protein aggregation in lyophilized formulations is also affected by the degree of change in protein conformation produced during the freeze-drying process (1). Greater changes in protein conformation are considered to lead to enhanced aggregation during subsequent storage.

In this study, the significance of local mobility in aggregation of lyophilized β-galactosidase (β-GA), a model protein, is discussed in comparison with the significance of structural relaxation and conformational changes. β-GA underwent significant inactivation during freeze drying with dextran, thus suggesting that significant conformational changes occurred during the process (13). When freeze dried with polyvinylalcohol or methylcellulose, inactivation was not observed during freeze drying (10). However, the time

[1] Division of Drugs, National Institute of Health Sciences, 1-18-1 Kamiyoga, Setagaya-ku, Tokyo 158-8501, Japan.
[2] To whom correspondence should be addressed. (e-mail: yoshioka@nihs.go.jp)

0724-8741/07/0900-1660/0

courses of aggregation during subsequent storage were describable with the empirical Kohlrausch-Williams-Watts (KWW) equation, thus leading to speculation that there were protein molecules having different conformations resulting from stresses during the freeze-drying process, each aggregating with a different time constant (10,14). The temperature dependence of the aggregation rate measured at the initial stage changed around T_{mc} (T_g determined by NMR relaxation measurement (15)), showing an apparent correlation between aggregation rate and structural relaxation (10). In this study, the significance of local obility in aggregation of lyophilized β-GA was examined in comparison with that of structural relaxation. The aggregation rates of β-GA lyophilized with trehalose, sucrose or stachyose were measured at temperatures near T_g, and correlations were examined between aggregation rate and local mobility (as measured by solid-state NMR), T_g (a primary parameter of structural relaxation), or protein conformational changes (as measured by FT-IR).

MATERIALS AND METHODS

Preparation of Lyophilized β-GA Formulations

β-GA from Aspergillus oryzae (10 U/mg; molecular weight: 105,000; isoelectric point:4.6) was kindly provided by Amano Enzyme Inc. (Nagoya, Japan) and purified by dialysis against 2.5 mM sodium phosphate solution of pH 4.5 (adjusted with HCl). After concentrated by ultrafiltration, trehalose (203-02252, Wako Pure Chemical Ind. Ltd, Osaka, Japan), sucrose (S-9378, Sigma Chemical Co., St. Louis, MO, USA) or stachyose (S-4001, Sigma Chemical Co., St. Louis, MO, USA) solution was added to make a 3.3 mg/ml β-GA solution with various weight fractions of excipient. Two hundred microliters of the solution was frozen in a polypropylene sample tube (2.0 ml) by immersion in liquid nitrogen for 10 min, and then dried at a vacuum level below 5 Pa for 23.5 h in a lyophilizer (Freezevac C-1, Tozai Tsusho Co., Tokyo, Japan). The shelf temperature was between −35 and −30°C for the first 10 h, 20°C for the subsequent 10 h, and 30°C for the last 3.5 h.

Determination of Water Sorption and T_g of Lyophilized β-GA Formulations

Water vapor absorption isotherms were measured gravimetrically at 25°C for lyophilized β-GA formulations containing trehalose, sucrose or stachyose using the automated sorption analyzer (MB-300 G system, VTI Corp., FL, USA). Samples were dried at 25°C under a vacuum level below 0.1 Pa until changes in weight were less than 1 μg per 10 min. Water contents of the samples at partial vapor pressures of 0.10 and 0.20 (corresponding to 10 and 20% relative humidity (RH), respectively) were determined based on equilibrated sample weight (changes in weight of less than 1 μg per 10 min).

The T_g of lyophilized β-GA formulations was determined by modulated temperature differential scanning calorimetry (2920; TA Instruments, DE, USA). Before T_g measurements, samples were stored at 15°C for 24 h in a desiccator with a saturated solution of $LiCl \cdot H_2O$ (12% RH). The conditions were as follows: modulation period of 100 s, a modulation amplitude of ±0.5°C, and an underlying heating rate of 1°C/min. Samples were put in a hermetic pan. Temperature calibration was performed using indium.

Determination of $T_{1\rho}$ of β-GA Carbonyl Carbon by ^{13}C Solid-state NMR

The rotating-frame spin-lattice relaxation time ($T_{1\rho}$) of β-GA carbonyl carbon in lyophilized formulations containing various weight fractions of trehalose, sucrose and stachyose was determined at 25°C using a UNITY plus spectrometer operating at a proton resonance frequency of 400 MHz (Varian Inc., CA, USA). Lyophilized samples were pre-equilibrated at 12% RH. Spin-locking field was equivalent to 19 kHz. The rotor size was 7 mm and spinning speed was 4 kHz. Peak height at approximately 180 ppm due to β-GA carbonyl carbon was followed with delay times of 1, 5, 10, 20, 30, 50 and 80 ms. Similar measurement of $T_{1\rho}$ was performed for lyophilized β-GA alone.

Fourier Transform Infra Red (FT-IR) Spectroscopy Measurements

FT-IR spectroscopy was performed using a JASCO FT/IR-6300 spectrometer (JASCO, Tokyo, Japan). A mixture of 100 mg KBr and 1–2 mg lyophilized β-GA formulation was pressed into a pellet under vacuum. A total of 256 scans and a resolution of 4 cm^{-1} were used for each spectrum. The second-derivative spectra were obtained from intact spectra without smoothing using Spectra Manager software version 2 (JASCO, Tokyo, Japan). The area of spectral absorbance was calculated using a baseline drawn between 1,600 and 1,700 cm^{-1}, and normalized for comparison between the formulations containing different excipients.

Determination of β-GA Aggregation Rate in Lyophilized Formulations

Lyophilized β-GA formulations containing trehalose, sucrose or stachyose, pre-equilibrated at 12% RH, were stored with a tight screw-cap at a constant temperature (40–90°C), removed at various times, and stored in liquid nitrogen until assayed. Samples were reconstituted in 1.7 ml of 200 mM phosphate buffer (pH 6.2), and injected into a size exclusion chromatography as described previously (10). The column (Tosoh G3000SW, 30 cm×7.5 mm, Tokyo) was maintained at 30°C, and 200 mM phosphate buffer (pH 6.2) was used as the mobile phase. The detection wavelength was 280 nm. Monomeric β-GA was determined based on the peak height of its chromatogram.

Reconstitution of lyophilized β-GA formulations after storage was also carried out using reconstitution mediums of 200 mM phosphate buffer (pH 6.2) containing 0.5% additives (dextran sulfate (197-08362, Wako Pure Chemical Ind. Ltd, Osaka, Japan), 2-hydroxylpropyl-β-cyclodextrin (C-0926, Sigma Chemical Co.), poly-L-lysine (P-7890, Sigma Chemical Co.), or pluronic (F-68, P-7061, Sigma Chemical Co., St. Louis, MO, USA).

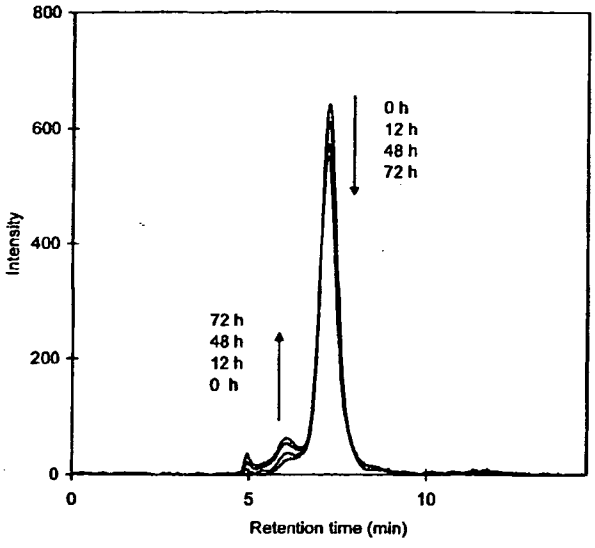

Fig. 1. Size-exclusion chromatograms of β-GA lyophilized with trehalose after various periods of storage at 80°C and 12%RH. The weight fraction of trehalose : 0.5.

RESULTS AND DISCUSSION

Aggregation of β-GA during Storage of Lyophilized Formulations

Figure 1 shows representative size-exclusion chromatograms of β-GA in lyophilized formulations, indicating that monomeric β-GA aggregates to larger sizes during storage. Tables I and II show the effects of reconstitution medium on the amount of monomeric β-GA remaining after storage of the formulation containing trehalose at temperatures below and above T_g, respectively. The amount of monomeric β-GA was not significantly affected by the addition of dextran sulfate or poly-L-lysine. Addition of pluronic also had no significant effect on the amount of monomeric β-GA. For lyophilized interleukin-2, the amount of aggregates after reconstitution was decreased by addition of poly-ions with high charge density, such as dextran sulfate and poly-L-lysine, and increased by addition of surfactants, such as pluronic, into the reconstitution buffer solution (16). This may be explained by assuming that the formation of aggregates from partially unfolded intermediates, as well as the reverse formation of native protein from intermediates, occur during the reconstitution process. In contrast, the lack of the effects of additives observed for β-GA aggregation indicates that neither formation of aggregates nor reverse formation of native protein from partially unfolded intermediates occurs during the reconstitution process. This finding suggests that β-GA aggregation occurs during the storage of lyophilized formulations, even at temperatures below T_g. Because large-scale diffusion of protein molecules is considered to be very limited in glassy solids, β-GA aggregation is considered to occur between protein molecules that are adjacent to each other without large-scale diffusion.

Temperature Dependence of β-GA Aggregation Rate

Figure 2 shows time courses of aggregation of β-GA at 50°C (below T_g) for lyophilized formulations with an excipient fraction of 0.33, and at 80°C (above T_g) for lyophilized formulations with an excipient fraction of 0.5. Similar time courses were obtained for formulations with various excipient fractions and at various temperatures. The wide range of the time courses could be better described by the KWW equation, but the initial stages of aggregation were describable with first-order kinetics. The solid line in Fig. 2 represents the theoretical time course of first-order kinetics.

The time required for 10% degradation (t_{90}) was calculated from the apparent first-order rate constant. Figure 3 shows the temperature-dependence of t_{90} determined for aggregation of β-GA lyophilized with sucrose, trehalose or stachyose at an excipient fractions of 0.33 and 0.5, 12% RH and various temperatures. For the sucrose and trehalose formulations, the temperature dependence of t_{90} exhibited a change in the slope at around T_g, suggesting significant effects of molecular mobility. For the stachyose formulation, the change in the slope was not obvious, because few data were available at temperatures above T_g. The values of t_{90} at T_g largely depended on the excipient; sucrose > trehalose > stachyose. The finding that the t_{90} values at T_g varied significantly between these three formulations suggests that β-GA aggregation rate is not primarily related to $(T-T_g)$.

Table I. Effects of Reconstitution Medium on β-GA Aggregation Below T_g for 0.09 Trehalose Formulation

Additives in Reconstitution Medium	Peak Height for Monomeric β-GA (Relative to Solution Prior to Freeze Drying)			
	After Freeze Drying		After 24 h-storage at 70°C	
None	0.97	(0.01)	0.65	(0.01)
Dextran Sulfate	0.96	(0.00)	0.62	(0.01)
2-hydroxylpropyl-β-cyclodextrin	0.95	(0.01)	0.62	(0.00)
Poly-L-lysine	0.94	(0.01)	0.62	(0.00)
Pluronic	0.97	(0.01)	0.66	(0.01)

0.5% additives
Values in brackets represent standard deviation (n=3)

Table II. Effects of Reconstitution Medium on β-GA Aggregation Above T_g for 0.33 Trehalose Formulation

Additives in Reconstitution Medium	Peak Height for Monomeric β-GA (Relative to Solution Prior to Freeze Drying)			
	After Freeze Drying		After 9 h-storage at 90°C	
None	0.99	(0.01)	0.74	(0.03)
Dextran Sulfate	1.00	(0.00)	0.74	(0.01)
2-hydroxylpropyl-β-cyclodextrin	0.98	(0.00)	0.73	(0.01)
Poly-L-lysine	0.98	(0.01)	0.74	(0.01)
Pluronic	1.00	(0.01)	0.76	(0.02)

0.5% additives
Values in brackets represent standard deviation (n=3)

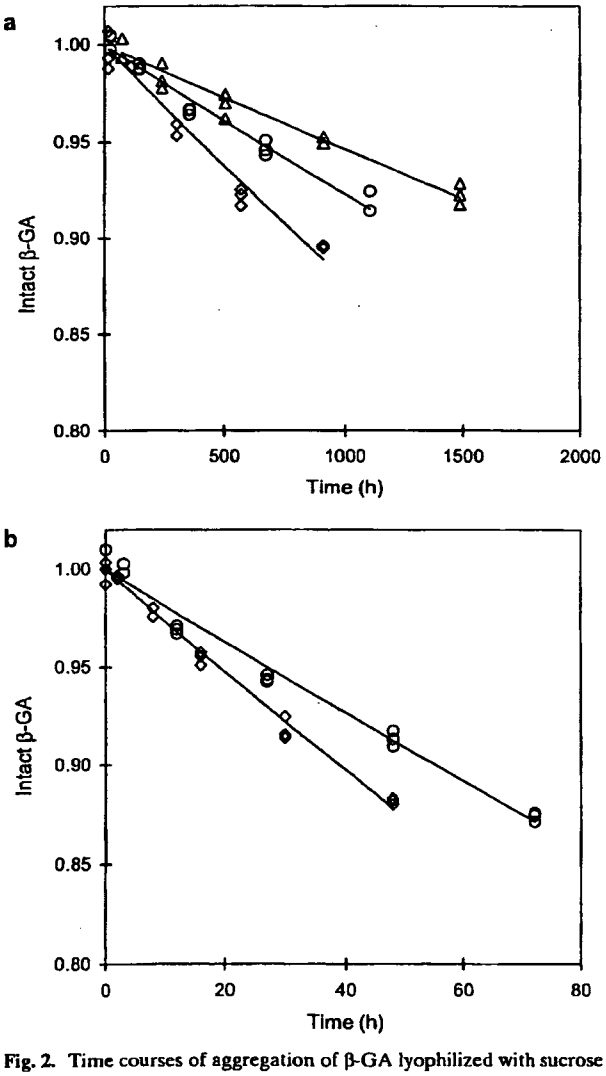

Fig. 2. Time courses of aggregation of β-GA lyophilized with sucrose (△), trehalose (O) or stachyose (◇). (a) aggregation at 50°C and excipient fraction of 0.33. (b) aggregation at 80°C and excipient fraction of 0.5.

Excipient-Fraction Dependence of β-GA Aggregation Rate

Figure 4 shows the dependence of t_{90} on the weight fraction of excipient at temperatures below T_g (50°C) and above T_g (80°C). As the weight fraction of excipient increased, t_{90} increased for all formulations. The values of t_{90} for the sucrose formulation in the amorphous state could not be determined at fractions above 0.5 at 50°C or above 0.33 at 80°C, because crystallization occurred during storage (crystallization was confirmed by the lack of crystallization peak in DSC thermograms). The t_{90} observed for β-GA aggregation showed a log-linear dependence on the excipient fraction, as reported for other proteins (11,12).

Figure 5 shows the water content and T_g determined for the lyophilized β-GA formulations with various weight fractions of trehalose, sucrose or stachyose. It has often been reported that lyophilized proteins without excipients do not show a distinct change in heat capacity in DSC thermograms. The T_g of lyophilized β-GA alone could not be determined in the dry state, but it could be estimated at 12% RH from small changes in heat capacity (Fig. 6). The T_g value determined at 12% RH depended on the excipient fraction (Fig. 5); T_g decreased with increasing excipient fraction from 0 to 0.3. Only a single T_g was observed in the range of excipient fractions from 0 to 0.3 for all formulations, suggesting that these formulations are a single glassy phase on levels detectable by DSC.

As shown in Figs. 4 and 5, the rank order of t_{90} at a certain excipient fraction was sucrose > trehalose > stachyose, whereas that of T_g of β-GA formulations was sucrose < trehalose < stachyose. The value of t_{90} increased significantly with increasing excipient fraction, even at small excipient fractions, in which T_g decreased significantly with increasing excipient fraction. These findings indicate that β-GA aggregation rate is not primarily related to $(T-T_g)$.

Figure 7 shows the amount of monomeric β-GA remaining after freeze drying with sucrose, trehalose or stachyose. Significant changes were observed at an excipient fraction of 0.09 for all formulations. The stachyose formulation exhibited the largest degree of β-GA aggregation during freeze drying. This finding suggests that freeze-drying processes cause changes in protein conformation at differing degrees between excipients, which in turn leads to the differences in β-GA aggregation rate observed between excipients. FT-IR is known to be useful for detecting changes in protein conformation produced during the freeze-drying process (17). Figure 8 compares the second derivative FT-IR

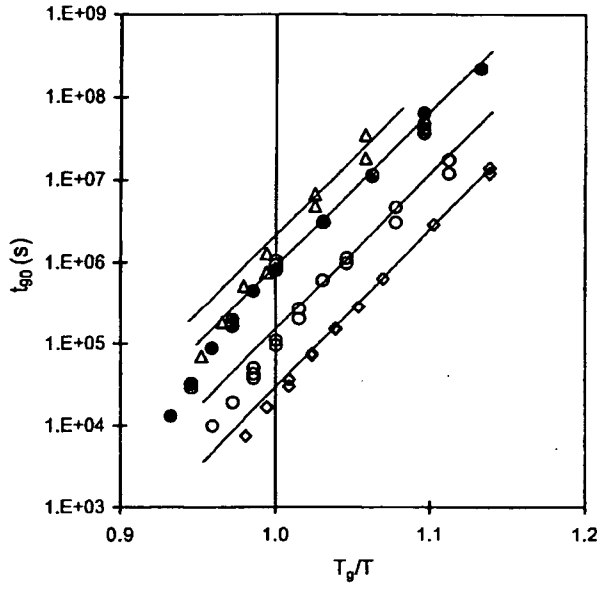

Fig. 3. T/T_g-dependence of t_{90} for aggregation of β-GA lyophilized with sucrose (△), trehalose (○●) or stachyose (◇). The weight fraction of excipient : 0.33 (△○◇) and 0.5 (●).

spectra between the sucrose, trehalose and stachyose formulations. Significant differences in spectra were not observed between the excipients, and the differences in β-GA aggregation rate observed between the excipients could not be attributed to differences in protein secondary structure. It is known that changes in the tertiary structure of protein molecules created during freeze-drying processes can lead to

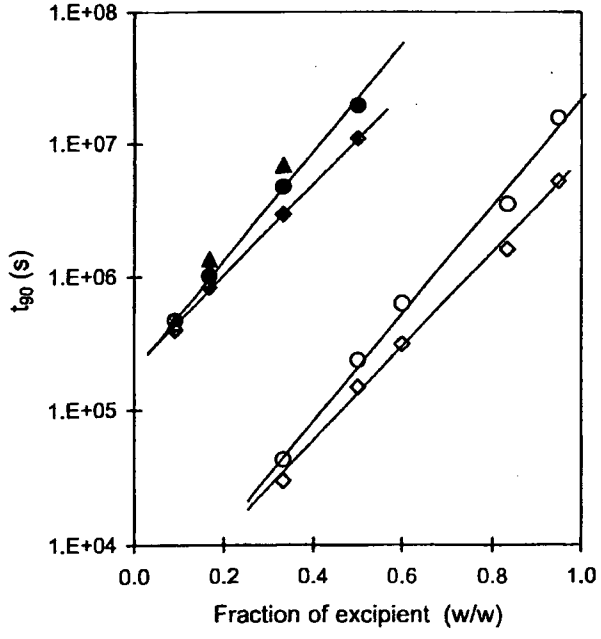

Fig. 4. Dependence of t_{90} on the weight fraction of excipient. The value of t_{90} was determined at 80°C and 12%RH for trehalose (○) and stachyose (◇), and at 50°C and 12%RH for trehalose (●), sucrose (▲) and stachyose (◆).

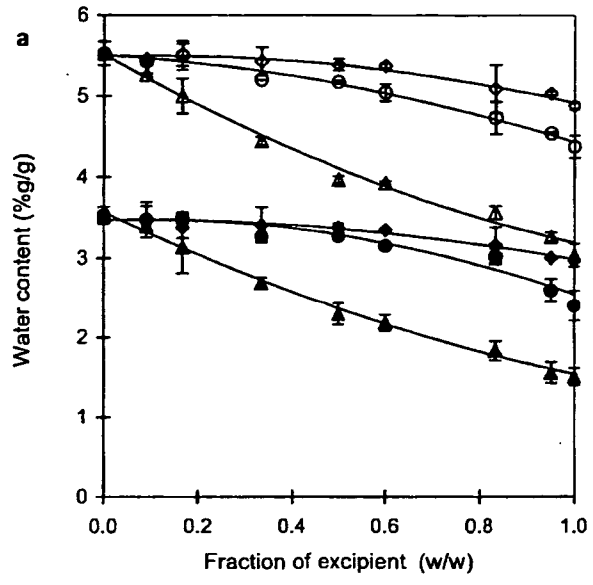

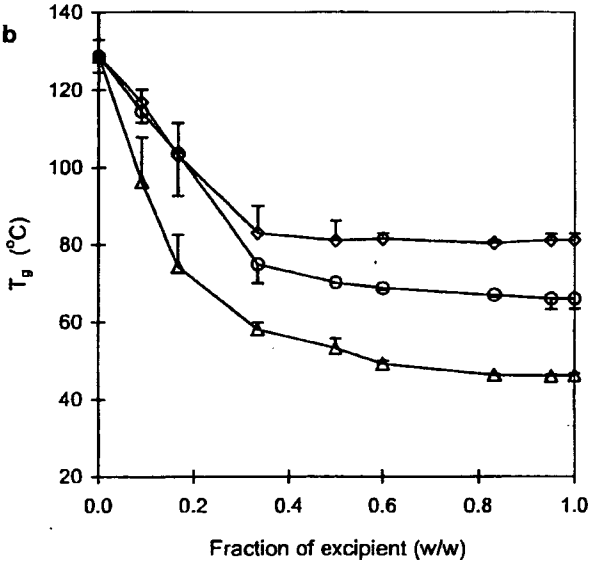

Fig. 5. Water content (a) and T_g (b) of lyophilized β-GA formulations containing trehalose (○●), sucrose (△▲), or stachyose (◇◆) as a function of the weight fraction of excipient. (a) *closed symbols*: 10%RH; *open symbols*: 20%RH. 25°C. (b) 12%RH. sd (n=3).

protein aggregation during storage. A possibility that a tertiary structural change is responsible for the differences in β-GA aggregation rate observed between the excipients cannot be excluded.

Significance of Local Mobility, as Determined by $T_{1\rho}$ of β-GA Carbonyl Carbon, and Structural Relaxation in Protein Aggregation

It is generally considered that the rate of protein aggregation, an intermolecular reaction, is mainly determined by structural relaxation that allows for large-scale

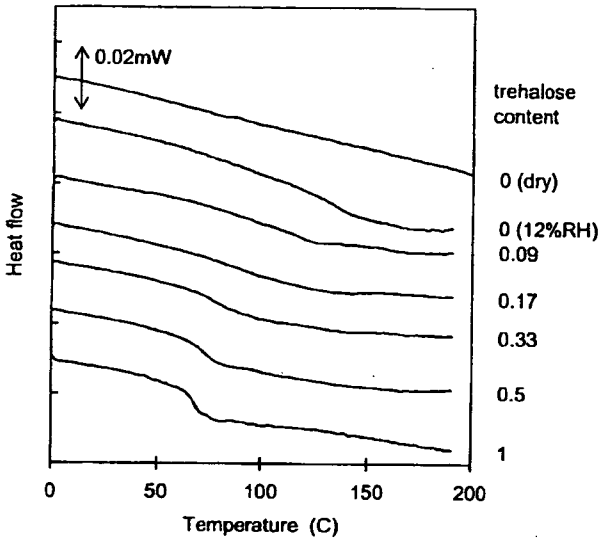

Fig. 6. DSC thermogram for β-GA lyophilized with various weight fractions of trehalose.

diffusion of reactants. From the finding that the t_{90} versus T_g/T plots for the lyophilized β-GA formulations exhibited a change in slope around T_g, β-GA aggregation rate appeared to correlate with structural relaxation. Although β-GA aggregation rate was not related to $(T-T_g)$, this may be explained by assuming that the fragility and fictive temperature of the formulation vary with the excipient. Because the structural relaxation times of the β-GA formulations were not determined in this study, correlations between β-GA aggregation rate and structural relaxation could not be elucidated.

Meanwhile, the local mobility of β-GA was determined by $T_{1\rho}$ of β-GA carbonyl carbon. Figure 9 shows the time course of rotating-frame spin-lattice relaxation at 25°C and 12% RH for the carbonyl carbon of β-GA lyophilized with sucrose, trehalose or stachyose at an excipient fraction of 0.5.

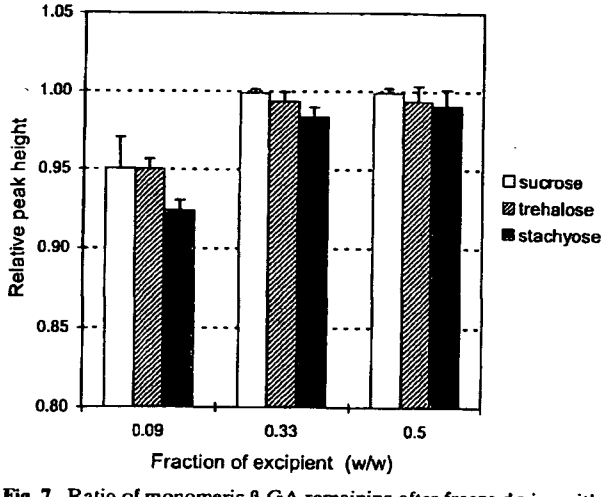

Fig. 7. Ratio of monomeric β-GA remaining after freeze drying with sucrose, trehalose or stachyose. *Bars* represent standard deviation (n=3).

Spin-lattice relaxation was significantly retarded by the addition of excipient. Sucrose resulted in the largest degree of retardation, and there were no significant differences in the degree of retardation between the trehalose and stachyose formulations. The time course of spin-lattice relaxation was describable with a bi-exponential equation including two different $T_{1\rho}$ values. The longer $T_{1\rho}$ value was estimated by curve fitting using a shorter $T_{1\rho}$ of 9 ms and a proportion of 13% for carbonyl carbons with the shorter $T_{1\rho}$. Figure 10 shows the estimates for the longer $T_{1\rho}$ of the dominating proportion, plotted as a function of the excipient fraction. The $T_{1\rho}$ for the sucrose formulation increased significantly with excipient fraction. For the stachyose formulation, in contrast, increases in $T_{1\rho}$ were not significant at an excipient fraction of 0.09, and $T_{1\rho}$ was less than in the sucrose formulation at higher excipient fractions. $T_{1\rho}$ for the trehalose formulation exhibited intermediate behavior when compared to the sucrose and stachyose formulations. The rank order of the ability of excipients to decrease the local

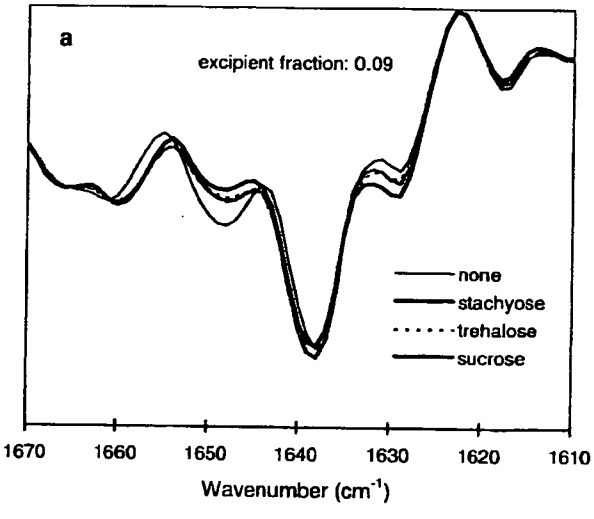

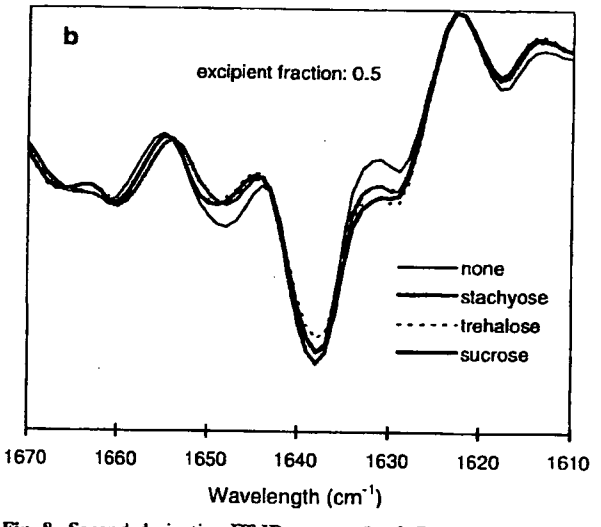

Fig. 8. Second derivative FT-IR spectra for β-GA lyophilized with sucrose, trehalose or stachyose of 0.09 (a) and 0.5 fractions (b).

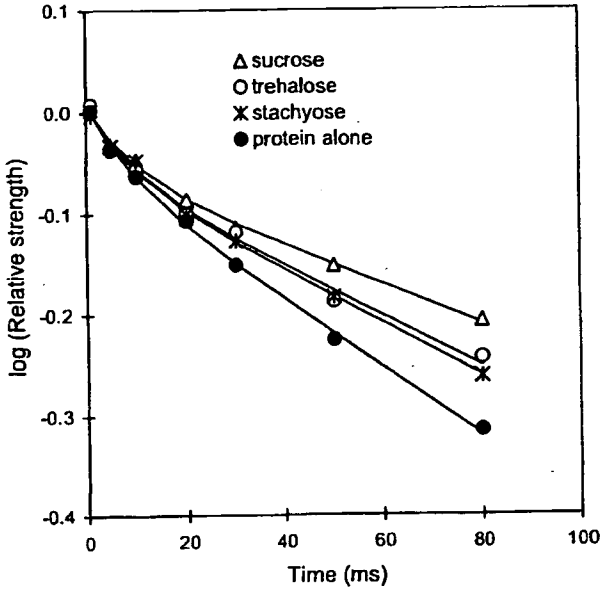

Fig. 9. Time course of spin-lattice relaxation at 25°C and 12%RH for carbonyl carbon of β-GA lyophilized with sucrose, trehalose or stachyose. The weight fraction of excipient : 0.5.

mobility of β-GA appeared to be the same as the rank order of their ability to decrease aggregation rate. This finding suggests that local mobility is a primary factor that affects the stability of lyophilized β-GA formulations; sucrose more potently inhibits local mobility of β-GA, and thus more strongly inhibits β-GA aggregation.

Local mobility is generally considered to follow Arrhenius kinetics. If local mobility is mainly responsible for β-GA aggregation, the temperature dependence of t_{90} should not show a change in slope around T_g. The non-Arrhenius temperature dependence observed for the t_{90} of β-GA aggregation, which is considered to be governed by local mobility, may be explained by assuming that local mobility of protein is coupled with structural relaxation. For bovine serum γ-globulin, the local mobility of protein, as measured by the laboratory-frame spin-lattice relaxation time (T_1) of protein carbonyl carbon, exhibited Arrhenius temperature dependence when lyophilized without excipient (18). When lyophilized with dextran, in contrast, the local mobility of protein exhibited a change in the slope of temperature dependence around the T_{mc} (T_g determined by NMR relaxation measurement), as did local mobility of dextran, as measured by T_1 of dextran methine carbon. These findings suggested that the local mobility of protein was coupled with the structural relaxation of lyophilized solids. The same may be said for the local mobility of protein and structural relaxation of β-GA lyophilized with sucrose, trahalose or stachyose. The local mobility of β-GA may exhibit Arrhenius temperature dependence in the absence of excipient. Upon the addition of excipient, local mobility may become to be coupled with structural relaxation, and the temperature dependence of protein local mobility may become to deviate from Arrhenius behavior.

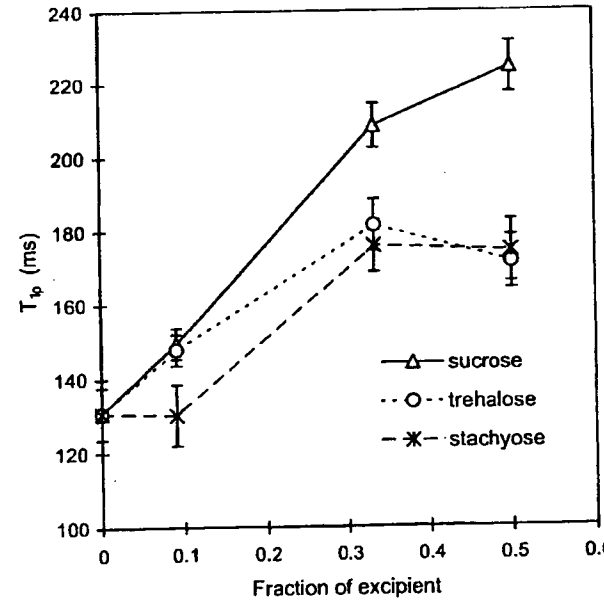

Fig. 10. Effect of weight fraction of excipient on $T_{1\rho}$ of carbonyl carbon at 25°C and 12%RH for β-GA lyophilized with sucrose, trehalose or stachyose

The great increase in t_{90} with increasing excipient fraction observed for β-GA aggregation rate, as indicated by log-linear dependence on the excipient fraction, may be attributed mainly to the effect of excipient inhibiting protein local mobility in addition to the effect of excipient diluting protein molecules.

CONCLUSION

The aggregation rate of β-GA lyophilized with sucrose, trehalose or stachyose unexpectedly correlated with the local mobility of β-GA rather than with ($T-T_g$). An increase in the weight fraction of excipient appeared to increase the effects of excipient decreasing local mobility, resulting in increases in the stability of β-GA. Sucrose exhibited the most intense stabilizing effect due to the most intense ability to inhibit local protein mobility during storage.

REFERENCES

1. M. J. Pikal. Chemistry in solid amorphous matrices: implication for biostabilization. In H. Levine (ed.), *Amorphous Food and Pharmaceutical Systems*, The Royal Society of Chemistry, Cambridge, UK, 2002, pp. 257–272.
2. S. Yoshioka, and Y. Aso. Correlations between molecular mobility and chemical stability during storage of amorphous pharmaceuticals. *J. Pharm. Sci.* in press (2006).
3. M. J. Pikal, K. M. Dellerman, M. L. Roy, and R. M. Riggin. The effects of formulation variables on the stability of freeze-dried human growth hormone. *Pharm. Res.* 8:427–436 (1991).
4. C. Schebor, M. P. Buera, and J. Chirife. Glassy state in relation to thermal inactivation of the enzyme invertase in amorphous dried matrices of trehalose, maltodextrin and PVP. *J. Food Eng.* 30:269–282 (1996).
5. S. J. Prestrelski, K. A. Pikal, and T. Arakawa. Optimization of lyophilization conditions for recombinant human interleukin-2

by dried-state conformational analysis using fourier-transform infrared spectroscopy. *Pharm. Res.* **12**:1250–1259 (1995).
6. S. Yoshioka, Y. Aso, and S. Kojima. Dependence of molecular mobility and protein stability of freeze-dried γ-globulin formulations on the molecular weight of dextran. *Pharm. Res.* **14**:736–741 (1997).
7. S. P. Duddu, and P. R. Dal Monte. Effect of glass transition temperature on the stability of lyophilized formulations containing a chimeric therapeutic monoclonal antibody. *Pharm. Res.* **14**:591–595 (1997).
8. S. Yoshioka, Y. Aso, and S. Kojima. Determination of molecular mobility of lyophilized bovine serum albumin and γ-globulin by solid state ^{1}H-NMR and relation to aggregation-susceptibility. *Pharm. Res.* 13:926–930 (1996).
9. S. Yoshioka, Y. Aso, and S. Kojima. Softening temperature of lyophilized bovine serum albumin and γ-globulin as measured by spin-spin relaxation time of protein protons. *J. Pharm. Sci.* **86**:470–474 (1997).
10. S. Yoshioka, S. Tajima, Y. Aso, and S. Kojima. Inactivation and aggregation of β-galactosidase in lyophilized formulation described by Kohlrausch-Williams-Watts stretched exponential function. *Pharm. Res.* **20**:1655–1660 (2003).
11. L. Chang, D. Shepherd, J. Sun, D. Ouellette, K. L. Grant, X. Tang, and M. J. Pikal. Mechanism of protein stabilization by sugars during freeze-drying and storage: native structure preservation, specific interaction, and/or immobilization in a glassy matrix? *J. Pharm. Sci.* **94**:1427–1444 (2005).
12. L. Chang, D. Shepherd, J. Sun, X. Tang, and M. J. Pikal. Effect of sorbitol and residual moisture on the stability of lyophilized antibodies: implications for the mechanism of protein stabilization in the solid state. *J. Pharm. Sci.* **94**:1445–1455 (2005).
13. S. Yoshioka, Y. Aso, S. Kojima, and T. Tanimoto. Effect of polymer excipients on the enzyme activity of lyophilized bilirubin oxidase and β-galactosidase formulations. *Chem. Pharm. Bull.* **48**:283–285 (2000).
14. S. Yoshioka, Y. Aso, and S. Kojima. Usefulness of Kohlrausch-Williams-Watts stretched exponential function to describe protein aggregation in lyophilized formulations and temperature dependence of near the glass transition temperature. *Pharm. Res.* 18:256–260 (2001).
15. S. Yoshioka, Y. Aso, and S. Kojima. The effect of excipients on the molecular mobility of lyophilized formulations, as measured by glass transition temperature and NMR relaxation-based critical mobility temperature. *Pharm. Res.* **16**:135–140 (1999).
16. M. Z. Zhang, K. Pikal, T. Nguyen, T. Arakawa, and S. J. Prestrelski. The effect of the reconstitution medium on aggregation of lyophilized recombinant interleukin-2 and ribonuclease A. *Pharm .Res.* **13**:643–646 (1996).
17. S. J. Prestrelski, T. Arakawa, and J. Carpenter. Separation of freezing- and drying-induced denaturation of lyophilized proteins using stress-specific stabilization. *Arch. Biochem. Biophys.* **303**:465–473 (1993).
18. S. Yoshioka, Y. Aso, S. Kojima, S. Sakurai, T. Fujiwara, and H. Akutsu. Molecular mobility of protein in lyophilized formulations linked to the molecular mobility of polymer excipients, as determined by high resolution ^{13}C solid-state NMR. *Pharm. Res.* **16**:1621–1625 (1999).

Available online at www.sciencedirect.com
ScienceDirect
International Journal of Pharmaceutics 336 (2007) 191–195
INTERNATIONAL JOURNAL OF PHARMACEUTICS
www.elsevier.com/locate/ijpharm

Note

Crystallization rate of amorphous nifedipine analogues unrelated to the glass transition temperature

Tamaki Miyazaki *, Sumie Yoshioka, Yukio Aso, Toru Kawanishi

National Institute of Health Sciences, 1-18-1 Kamiyoga, Setagaya-ku, Tokyo 158-0851, Japan

Received 14 August 2006; received in revised form 12 October 2006; accepted 18 November 2006
Available online 28 November 2006

Abstract

To examine the relative contributions of molecular mobility and thermodynamic factor, the relationship between glass transition temperature (T_g) and the crystallization rate was examined using amorphous dihydropyridines (nifedipine (NFD), *m*-nifedipine (*m*-NFD), nitrendipine (NTR) and nilvadipine (NLV)) with differing T_g values. The time required for 10% crystallization, t_{90}, was calculated from the time course of decreases in the heat capacity change at T_g. The t_{90} of NLV and NTR decreased with decreases in T_g associated with water sorption. The t_{90} versus T_g/T plots almost overlapped for samples of differing water contents, indicating that the crystallization rate is determined by molecular mobility as indicated by T_g. In contrast, differences in the crystallization rate between these four drugs cannot be explained only by molecular mobility, since the t_{90} values at a given T_g/T were in the order: NLV > NTR > NFD ≈ *m*-NFD. A lower rate was obtained for amorphous drugs with lower structural symmetry and more bulky functional groups, suggesting that these factors are also important. Furthermore, the crystallization rate of NTR in solid dispersions with poly(vinylpyrrolidone) (PVP) and hydroxypropyl methylcellulose (HPMC) decreased to a greater extent than expected from the increased T_g. This also suggests that factors other than molecular mobility affect the crystallization rate.

Keywords: Crystallization; Amorphous state; Nifedipine; Glass transition; Molecular mobility; Excipients

Preparation of poorly water-soluble pharmaceuticals into amorphous forms improves their solubility. However, amorphous solids are physically unstable because of their high energy state, and crystallization during storage presents a problem. The process of crystallization is known to comprise two major steps: nucleation and crystal growth, and the rates are generally governed by molecular mobility affecting the diffusion rate of molecules and thermodynamic factors such as the Gibbs free energy and nucleus/amorphous interfacial energy (Saleki-Gerhardt and Zografi, 1994; Hancock and Zografi, 1997; Rodríguez-Hornedo and Murphy, 1999; Andronis and Zografi, 2000; Ngai et al., 2000). Our previous studies demonstrated that the overall crystallization rate of nifedipine (NFD) for both the amorphous pure drug and solid dispersions with poly(vinylpyrrolidone) (PVP) had similar temperature dependence as the mean relaxation time calculated using the Adam-Gibbs-Vogel equation, suggesting that the molecular mobility of amorphous pharmaceuticals was one of the important factors affecting the crystallization rate (Aso et al., 2001, 2004). However, the crystallization rate of amorphous pharmaceuticals cannot be determined only by molecular mobility, as it has been reported that the susceptibility to crystallization of pharmaceuticals possessing quite different thermodynamic properties does not follow the order of the decrease in the glass transition temperature (T_g) (Zhou et al., 2002).

The purpose of the present study is to discuss the relative contributions of the molecular mobility and thermodynamic factors to the crystallization rates of dihydropyridines with different substituents, including NFD, *m*-nifedipine (*m*-NFD), nitrendipine (NTR) and nilvadipine (NLV) (Fig. 1). The overall crystallization rates of these drugs in the pure amorphous solids were measured under various relative humidity (RH) conditions to elucidate the effects of the substituents and water content on the crystallization rate. The crystallization rate of NTR was also determined in solid dispersions containing polymers (PVP and hydroxypropyl methylcellulose (HPMC)). Although some

* Corresponding author. Tel.: +81 3 3700 1141; fax: +81 3 3707 6950.
E-mail addresses: miyazaki@nihs.go.jp (T. Miyazaki), yoshioka@nihs.go.jp (S. Yoshioka), aso@nihs.go.jp (Y. Aso), kawanish@nihs.go.jp (T. Kawanishi).

0378-5173/$ – see front matter © 2006 Elsevier B.V. All rights reserved.
doi:10.1016/j.ijpharm.2006.11.052

	abbreviation	R_1	R_2	R_3	R_4
nifedipine	[NFD]	CH_3	CH_3	NO_2	H
m-nifedipine	[m-NFD]	CH_3	CH_3	H	NO_2
nitrendipine	[NTR]	CH_3	C_2H_5	H	NO_2
nilvadipine	[NLV]	CN	$(CH_3)_2CH$	H	NO_2

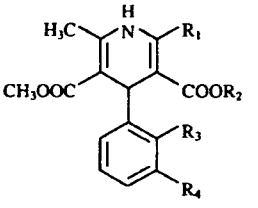

Fig. 1. Chemical structures of dihydropyridines.

papers have dealt with the crystallization of NTR and NLV in solid dispersions (Hirasawa et al., 2003a,b, 2004; Wang et al., 2005, 2006), few data are available that allow quantitative discussion about the relationship between molecular mobility and crystallization rates.

NFD and HPMC (USP grade) were purchased from Sigma Chemical Co. NTR, *m*-NFD and PVP (weight average molecular weight of 40000) were obtained from Wako Pure Chemical Industries Ltd. NLV was kindly supplied by Astellas Pharma Inc. The amorphous NFD, *m*-NFD, NTR, NLV and NTR solid dispersions with PVP and HPMC were prepared by melt quenching in the cell of a differential scanning calorimeter (DSC2920, TA Instruments). The crystalline drug or mixture of NTR and polymer (5 mg) was melted at a temperature approximately 20 °C above its melting point and then cooled to approximately 100 °C below the T_g at a cooling rate of 40 °C/min. Thermal and photo degradation of the drugs was checked by HPLC, and no change in the chromatograms was observed after the preparation in comparison with that before. Fig. 2 shows typical DSC thermograms for the four amorphous drugs immediately after preparation and after subsequent storage. The T_g values for the amorphous drugs were: NLV, 48.6 ± 0.3 °C; NFD, 46.2 ± 0.2 °C; *m*-NFD, 41.3 ± 0.1 °C; NTR, 32.4 ± 0.3 °C. As shown in Fig. 2(b), freshly prepared amorphous NFD exhibited two endothermic peaks at around 161 °C and 168 °C. The two melting points of the peaks agreed well with that for the metastable form II and stable form I, respectively (Burger and Koller, 1996). As shown in Fig. 2(c), the NFD sample, retaining an amorphous portion after 5 h storage at 60 °C, showed exothermic peaks due to crystallization of the amorphous phase and its transformation into a stable crystal, and melted at 168 °C, which is approximately the same temperature as the melting point of the intact crystal. As shown in Fig. 2(d), the sample stored at 60 °C for 46 h showed the exothermic peak around 120–140 °C due to transformation into a stable crystal, although change in the heat capacity (ΔC_p) at T_g was not significant. The exothermic peak around 120–140 °C due to transformation into a stable crystal was also observed during storage at 50 °C and 70 °C (thermogram not shown). These DSC thermograms suggested that amorphous NFD initially crystallized into a metastable form. Crystallization into the metastable form was also observed during storage at 50 °C and 70 °C (thermogram not shown). Amorphous *m*-NFD showed an exothermic peak due to crystallization but no obvious peak due to transformation into a stable form like that shown by the NFD samples, and melted at 206 °C, which is approximately the same temperature as the melting point of intact *m*-NFD (Fig. 2(f) and (g)). It is not clear from the DSC thermograms whether transition to a stable or a metastable crystalline form occurred during storage. Fig. 2(j) and (k) show the DSC thermograms of the partially crystallized NTR samples showing one melting peak at 128 °C. The observed melting point was lower than that of the stable crystal

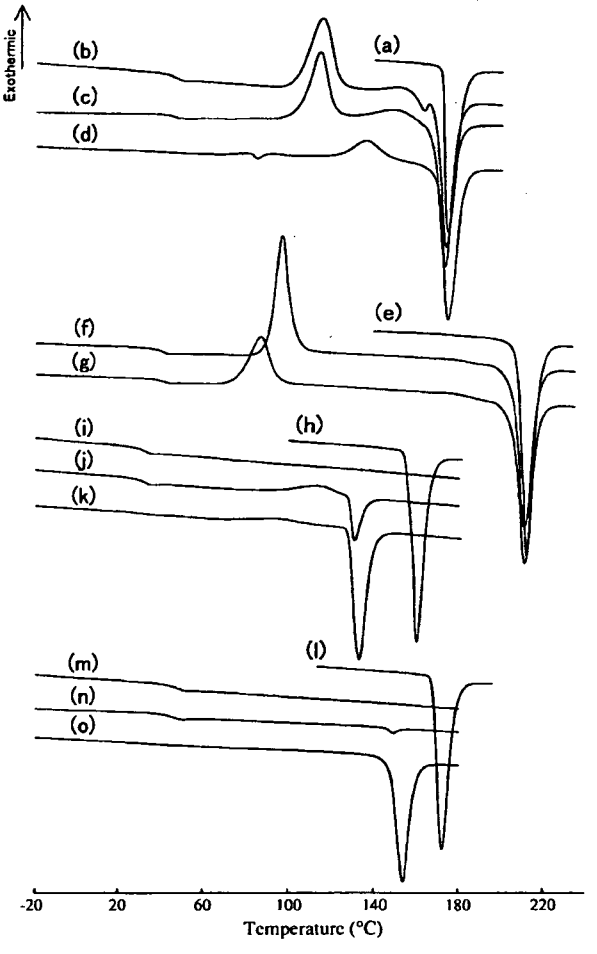

Fig. 2. Typical DSC thermograms: (a) NFD crystalline in the stable form, (b) freshly prepared amorphous NFD, (c) amorphous NFD after 5h-storage at 60 °C (d) amorphous NFD after 46 h-storage at 60 °C, (e) m-NFD crystalline in the stable form, (f) freshly prepared amorphous m-NFD, (g) amorphous m-NFD after 15 h-storage at 50 °C, (h) NTR crystalline in the stable form, (i) freshly prepared amorphous NTR, (j) amorphous NTR after 2 h-storage at 60 °C, (k) amorphous NTR after 9.75 h-storage at 60 °C, (l) NLV crystalline in the stable form, (m) freshly prepared amorphous NLV, (n) amorphous NLV after 48 h-storage at 80 °C, (o) amorphous NLV after 168 h-storage at 80 °C. Heating rate: 20 °C/min.

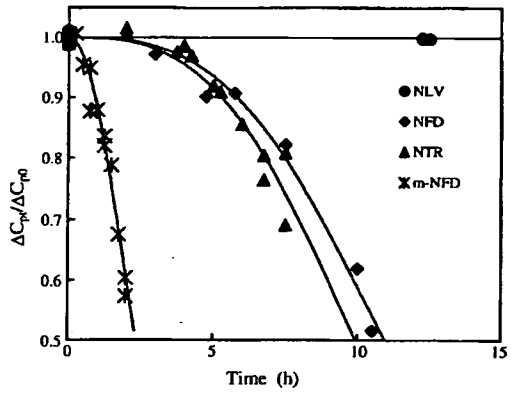

Fig. 3. Time profiles of crystallization for four dihydropyridines at 60 °C and 0%RH. The ratio of the amorphous form remaining at time t was calculated from the ΔC_p value assuming that the amount of amorphous phase is proportional to the ΔC_p. ΔC_{p0} and ΔC_{pt} are changes in ΔC_p at time 0 and t, respectively. Solid lines denote the fitting to the Avrami equation ($x(t) = \exp[-kt^n]$, $n = 3$).

(158 °C) and consistent with that reported for a metastable crystal (Kuhnert-Brandstätter and Völlenklee, 1986; Burger et al., 1997). As shown in Fig. 2(n) and (o), the partially crystallized NLV samples showed one melting peak at 148 °C. The observed melting point was lower than that for a stable crystal (168 °C) and similar to that for the dehydrated form of the monohydrate (Hirayama et al., 2000). Both amorphous NTR and NLV samples were considered to crystallize to their metastable crystalline forms under the conditions studied.

Fig. 3 shows the time profiles of crystallization of NFD, *m*-NFD, NTR, NLV at 60 °C and 0%RH. The crystallization rate was in the order: NLV < NTR = NFD < *m*-NFD. Fig. 4 shows the temperature dependence of the time required for 10% crystallization (t_{90}). Although NFD and NLV have approximately the same T_g, their values of t_{90} at the same temperature differed by more than two orders of magnitude (Fig. 4(A)). As shown in Fig. 4(B), the value of t_{90} at a given T_g/T (T being storage temperature) was in the order: NLV > NTR > NFD ≈ *m*-NFD within the whole range of temperature studied. As shown in Fig. 1, the four dihydropyridines have various alkyl groups at one of the carbonylester positions (R_2), and differ in the substitution position of the nitro group in the phenyl moiety (R_3 or R_4). The

Table 1
T_g values of amorphous NLV and NTR

RH (%)	T_g (°C)	
	NLV	NTR
0 (P_2O_5)	48.6 ± 0.3	32.4 ± 0.3
12 ($LiCl{\cdot}2H_2O$)	48.1 ± 0.7	30.5 ± 0.4
25 (CH_3COOK)	46.4 ± 0.5	29.0 ± 0.3
43 ($K_2CO_3{\cdot}2H_2O$)	43.4 ± 0.4	25.8 ± 0.3

For water absorption, the samples were kept at 5 °C for approximately 50 h in a desiccator containing saturated salt solutions. No crystallization was observed during the water absorption, as indicated by no endothermic melting peak in DSC thermograms.

bulkiness of R_2 shows the order: NFD, *m*-NFD (methyl) < NTR (ethyl) < NLV (isopropyl). Furthermore, the substituent at R_1 is a cyano group in NLV, whereas it is a methyl group in the other three drugs; thus, the structural symmetry of NLV is lower. Since the plots for NFD and *m*-NFD in Fig. 4(B) almost overlapped each other, the difference in the crystallization rate may be attributed to the difference in molecular mobility. In contrast, differences in the crystallization rate between NLV, NTR and NFD cannot be explained only by the difference in molecular mobility. The differences in structural symmetry and bulkiness of functional group may cause differences in the Gibbs free energy and nucleus/amorphous interfacial energy, resulting in the differing crystallization rates between these drugs.

The crystallization rate of amorphous NLV and NTR solids with differing T_g values due to differing water content was measured to elucidate the effect of T_g on the crystallization rate (Table 1). The partially crystallized NLV and NTR in the presence of water showed an endothermic melting peak at approximately 150 °C and 130 °C, respectively. This suggests that amorphous NLV and NTR containing water also crystallize into their metastable forms in a similar manner as shown for dry samples. Fig. 5(A) shows the temperature dependence of the t_{90} obtained for NLV and NTR in the presence of water. When compared at the same temperature, the t_{90} value decreased with increasing RH. As shown in Fig. 5(B), the t_{90} versus T_g/T plots for each drug overlapped with those obtained under dry conditions, suggesting that the effect of water on the t_{90} value was explainable by the plasticizing effect of absorbed water,

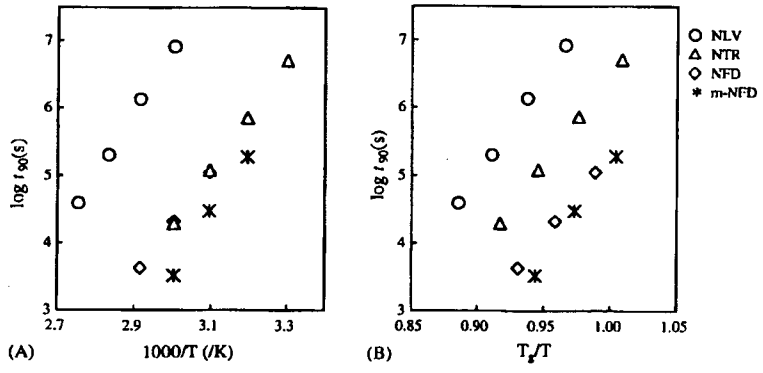

Fig. 4. Relationship between t_{90} for crystallization of drugs and storage temperature under dry conditions.

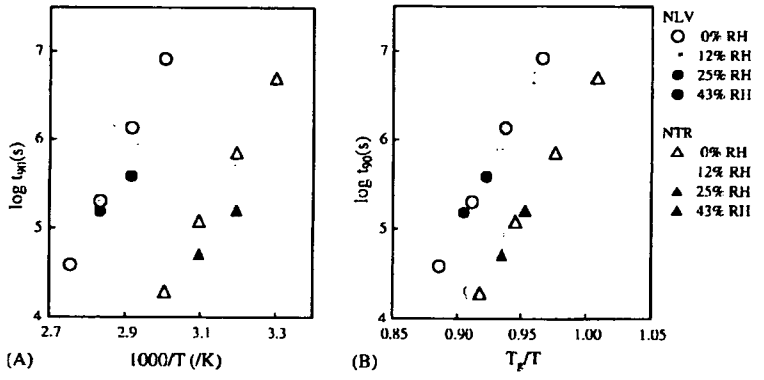

Fig. 5. Effect of absorbed water on the t_{90} of crystallization for NLV (circles) and NTR (triangles). The t_{90} values were measured at the early stage of crystallization at which no marked change in Tg was evident.

Table 2
T_g values of NTR-polymer solid dispersions

Polymer (%)	T_g (°C)	
	PVP	HPMC
0	32.4 ± 0.3	
3	33.2 ± 0.2	32.4 ± 0.1
5	34.1 ± 0.3	32.9 ± 0.4
6	34.1 ± 0.3	32.8 ± 0.2
11	36.6 ± 0.3	33.4 ± 0.3
20	–	33.7 ± 0.7
23	43.4 ± 0.8	–

similarly to that reported for NFD crystallization (Aso et al., 1995).

The effect of T_g on the crystallization rate of NTR was also investigated in solid dispersions with PVP and HPMC. A single T_g was observed for amorphous NTR-polymer solid dispersions prepared with 2.7–23% polymer excipients, indicating that NTR and polymer are miscible within the sensitivity limit of the DSC method. The value of T_g tended to increase with the amount of polymer, and the extent of increase was greater for NTR-PVP dispersions than for NTR-HPMC dispersions (Table 2). As the partially crystallized NTR-polymer dispersions showed a melt-

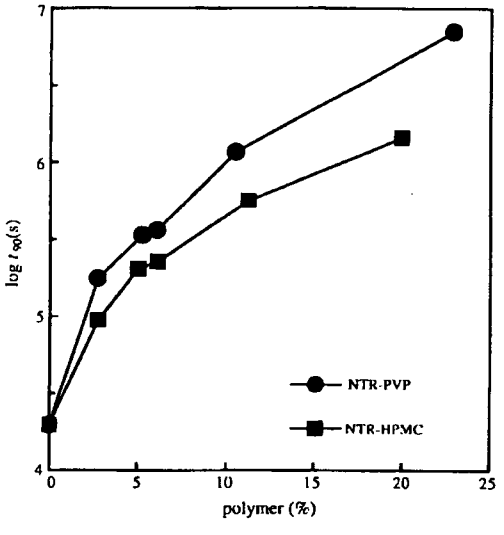

Fig. 6. Effect of polymer content on crystallization of NTR in solid dispersions with PVP and HPMC at 60 °C and 0%RH.

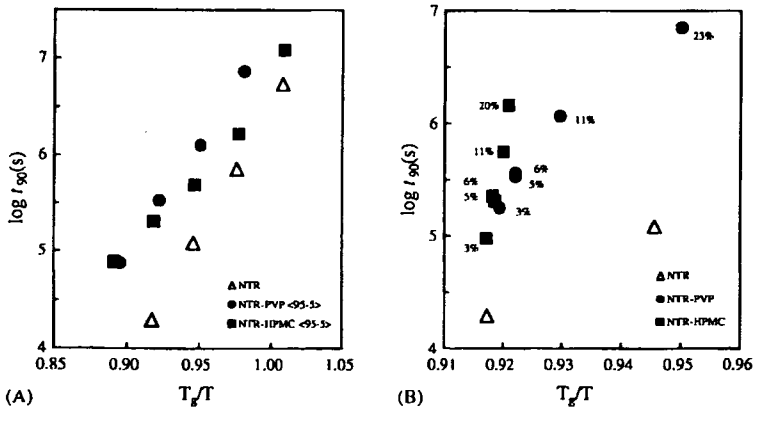

Fig. 7. Relationship between T_g/T and t_{90} of crystallization for NTR in the pure amorphous form and solid dispersions with PVP and HPMC. Numbers in percentage terms in figure (B) denote polymer contents.

ing peak at approximately 130 °C, the crystallization of NTR in the presence of the polymers was considered to be transition into a metastable form in a similar manner as that observed for pure amorphous NTR. Fig. 6 shows the effect of polymer excipients on the t_{90} values. Both PVP and HPMC increased t_{90} as the amount of polymer increased, but PVP was more effective in stabilizing amorphous NTR within the range of content studied. Fig. 7(A) shows the temperature dependence of t_{90} for solid dispersions containing 5% polymer. The t_{90} value compared at the same T_g/T was longer for both NTR-polymer dispersions than for pure NTR. Furthermore, the t_{90} versus T_g/T plots for solid dispersions containing various amounts of polymers did not overlap with that for pure NTR (Fig. 7(B)), indicating that crystallization of NTR was inhibited by the addition of PVP and HPMC to a greater extent than expected from the increased T_g. The present results imply that the drug-polymer interaction as well as an antiplasticizing effect of polymer excipients retarded the crystallization of the amorphous solid (Hirasawa et al., 2003a,b, 2004; Aso et al., 2004; Miyazaki et al., 2004, 2006; Wang et al., 2006).

Acknowledgement

A part of this work was supported by a grant from the Japan Health Science Foundation.

References

Andronis, V., Zografi, G., 2000. Crystal nucleation and growth of indomethacin polymorphs from the amorphous state. J. Non-Cryst. Solids 271, 236–248.

Aso, Y., Yoshioka, S., Otsuka, T., Kojima, S., 1995. The physical stability of amorphous nifedipine determined by isothermal microcalorimetry. Chem. Pharm. Bull. 43, 300–303.

Aso, Y., Yoshioka, S., Kojima, S., 2001. Explanation of the crystallization rate of amorphous nifedipine and Phenobarbital from their molecular mobility as measured by ^{13}C nuclear magnetic resonance relaxation time and the relaxation time obtained from the heating rate dependence of the glass transition temperature. J. Pharm. Sci. 90, 798–806.

Aso, Y., Yoshioka, S., Kojima, S., 2004. Molecular mobility-based estimation of the crystallization rates of amorphous nifedipine and Phenobarbital in poly(vinylpyrrolidone) solid dispersions. J. Pharm. Sci. 93, 384–391.

Burger, A., Koller, K.T., 1996. Polymorphism and pseudopolymorphism on nifedipine. Sci. Pharm. 64, 293–301.

Burger, A., Rollinger, J.M., Brüggeller, P., 1997. Binary system of (*R*)- and (*S*)-nitrendipine—polymorphism and structure. J. Pharm. Sci. 86, 674–679.

Hancock, B.C., Zografi, G., 1997. Characteristics and significance of the amorphous state in pharmaceutical systems. J. Pharm. Sci. 86, 1–12.

Hirasawa, N., Ishise, S., Miyata, H., Danjo, K., 2003a. Physicochemical characterization and drug release studies of Nilvadipine solid dispersions using water-insoluble polymer as a carrier. Drug Dev. Ind. Pharm. 29, 339–344.

Hirasawa, N., Ishise, S., Miyata, H., Danjo, K., 2003b. An attempt to stabilize Nilvadipine solid dispersion by the use of ternary systems. Drug Dev. Ind. Pharm. 29, 997–1004.

Hirasawa, N., Ishise, S., Miyata, H., Danjo, K., 2004. Application of Nilvadipine solid dispersion to tablet formulation and manufacturing using crospovidone and methylcellulose as dispersion carriers. Chem. Pharm. Bull. 52, 244–247.

Hirayama, F., Honjo, M., Arima, H., Okimoto, K., Uekama, K., 2000. X-ray crystallographic characterization of Nilvadipine monohydrate and its phase transition behavior. Eur. J. Pharm. Sci. 11, 81–88.

Kuhnert-Brandstätter, M., Völlenklee, R., 1986. Beitrag zur polymorphie von arzneistoffen 2. Mitteilung: halofenat, lorcainidhydrochlorid, minoxidil, mopidamol und nitrendipin. Sci. Pharm. 54, 71–82.

Miyazaki, T., Yoshioka, S., Aso, Y., Kojima, S., 2004. Ability of polyvinylpyrrolidone and polyacrylic acid to inhibit the crystallization of amorphous acetaminophen. J. Pharm. Sci. 93, 2710–2717.

Miyazaki, T., Yoshioka, S., Aso, Y., 2006. Physical stability of amorphous acetanilide derivatives improved by polymer excipients. Chem. Pharm. Bull. 54, 1207–1210.

Ngai, K.L., Magill, J.H., Plazek, D.J., 2000. Flow, diffusion and crystallization of supercooled liquids: revisited. J. Chem. Phys. 112, 1887–1892.

Rodríguez-Hornedo, N., Murphy, D., 1999. Significance of controlling crystallization mechanisms and kinetics in pharmaceutical systems. J. Pharm. Sci. 88, 651–660.

Saleki-Gerhardt, A., Zografi, G., 1994. Non-isothermal and isothermal crystallization of sucrose from the amorphous state. Pharm. Res. 11, 1166–1173.

Wang, L., Cui, F.D., Hayase, T., Sunada, H., 2005. Preparation and evaluation of solid dispersion for Nitrendipine-carbopol and Nitrendipine-HPMCP systems using a twin screw extruder. Chem. Pharm. Bull. 53, 1240–1245.

Wang, L., Cui, F.D., Sunada, H., 2006. Preparation and evaluation of solid dispersions of Nitrendipine prepared with fine silica particles using the melt-mixing method. Chem. Pharm. Bull. 54, 37–43.

Zhou, D., Zhang, G.G.Z., Law, D., Grant, K.J.W., Schmitt, E.A., 2002. Physical stability of amorphous pharmaceuticals: importance of configurational thermodynamic quantities and molecular mobility. J. Pharm. Sci. 91, 1863–1872.

J Pharmacol Sci 104, 397 – 401 (2007)

Journal of Pharmacological Sciences

Short Communication

Involvement of Intracellular Ca^{2+} in the Regulatory Volume Decrease After Hyposmotic Swelling in MDCK Cells

Naoko Iida-Tanaka[1], Iyuki Namekata[2], Megumi Kaneko[1], Miku Tamura[2], Toru Kawanishi[3], Ryu Nakamura[4], Koki Shigenobu[2], and Hikaru Tanaka[2,*]

[1]*Department of Food Science, Faculty of Home Economics, Otsuma Woman's University, Chiyoda-ku, Tokyo 102-8357, Japan*
[2]*Department of Pharmacology, Toho University Faculty of Pharmaceutical Sciences, Funabashi, Chiba 274-8510, Japan*
[3]*Division of Drugs, National Institute of Health Sciences, Setagaya-ku, Tokyo 158-8501, Japan*
[4]*Advanced Imaging Microscopy Department, Product Management Division of Microscopy, Carl Zeiss Tokyo, Shinjuku-ku, Tokyo 160-0003, Japan*

Received January 24, 2007; Accepted June 14, 2007

Abstract. We examined the source of Ca^{2+} involved in the volume regulation of Madin-Darby canine kidney (MDCK) cells with confocal microscopy and fluoroprobes. Hyposmosis induced a transient increase in cell volume, as well as cytoplasmic Ca^{2+}, which peaked at 3 to 5 min and gradually decreased to reach the initial value within about 30 min. This late decrease in cell volume, as well as the transient rise in cytoplasmic Ca^{2+}, was reduced in Ca^{2+}-free solution and was abolished by pretreatment with thapsigargin. In conclusion, Ca^{2+} released from the intracellular store contributes to the regulatory volume decrease following hyposmotic swelling in MDCK cells.

Keywords: hyposmosis, cell volume, intracellular Ca^{2+}

Although the composition of blood plasma is strictly regulated under physiological conditions, the cells in the body may experience anisosmolarity under pathological conditions such as ischemia, septic shock, and diabetic coma. The ability of cells to restore cell volume under such a condition may be crucial to their survival. Cells of various organs in the body including the heart, brain, kidney, bladder, liver, and skeletal muscle possess mechanisms for restoring cell volume under osmotic challenge and can reverse the swelling effect of hyposmosis and the shrinking effect of hyperosmosis (1).

Madin-Darby canine kidney (MDCK) cells originate from the renal distal tubular epithelium. In this cell line, the key players of water and ion transport such as aquaporins and ion channels are expressed (2, 3), and responsiveness to humoral regulatory substances such as vasopressin is well maintained (4). Thus, MDCK cells have been widely used as a model to study volume regulation of renal epithelial cells. We have reported that over-expression of sulfoglycolipids confers resistance against hyper- and hypotonic stresses to MDCK cells (5). Following hyposmotic challenge, the volume of MDCK cells are known to increase within a few minutes, which is followed by a decrease towards the initial value under hyposmotic conditions (6, 7), a process known as regulatory volume decrease (8, 9). Activation of ion channels such as potassium and chloride channels have been reported and some of these processes are postulated to be triggered by a rise in cytoplasmic Ca^{2+} concentration. However, the source of Ca^{2+} responsible for the rise has not been clarified. In the present study, we performed measurements of the cell volume and cytoplasmic Ca^{2+} in MDCK cells by confocal and epifluorescent microscopy to determine the significance and source of Ca^{2+} in the regulatory volume decrease under persistent hyposmotic conditions.

MDCK cells (National Institute of Health Science) were cultured in Eagles Modified Essential Medium (EMEM) supplemented with 1% penicillin and 0.4% streptomycin. The transformants were plated on glass coverslips 48 to 72 h before the experiments. At 1 h before the experiments, the coverslips were placed in a

*Corresponding author. htanaka@phar.toho-u.ac.jp
Published online in J-STAGE: August 10, 2007
doi: 10.1254/jphs.SC0070024